

# UNCLASSIFIED

AD NUMBER
AD871971
NEW LIMITATION CHANGE
TO Approved for public release, distribution unlimited
FROM Distribution authorized to U.S. Gov't. agencies and their contractors; Critical Technology; JUN 1979. Other requests shall be referred to Rome Air5 Development Center, AFSC, Griffiss AFB, NY.
AUTHORITY
RADC USAF ltr, 16 Sep 1971

THIS PAGE IS UNCLASSIFIED

AD871971

AD No. \_\_\_\_\_  
FILE COPY

RADC-TR-70-96  
Final Technical Report  
June 1970



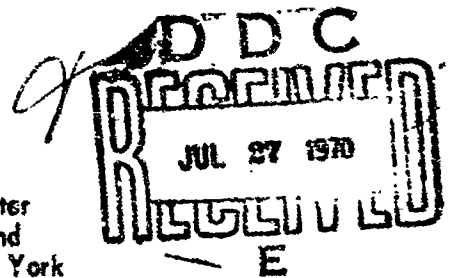
29  
CB

# FIELD EFFECT LIQUID CRYSTAL

RCA Corporation

This document is subject to special export controls and each transmittal to foreign governments or foreign nationals may be made only with prior approval of RADC (EMBDE), GAFE, NY 13440.

Rome Air Development Center  
Air Force Systems Command  
Griffiss Air Force Base, New York



When US Government drawings, specifications, or other data are used for any purpose other than a definitely related government procurement operation, the government thereby incurs no responsibility nor any obligation whatsoever; and the fact that the government may have formulated, furnished, or in any way supplied the said drawings, specifications, or other data is not to be regarded, by implication or otherwise, as in any manner licensing the holder or any other person or corporation, or conveying any rights or permission to manufacture, use, or sell any patented invention that may in any way be related thereto.

NOTED BY	
DATE	PRINT SECTION <input type="checkbox"/>
SEC	SOFT SECTION <input checked="" type="checkbox"/>
CHANGES	<input checked="" type="checkbox"/>
JUSTIFICATION	
BY	
DISTRIBUTION/AVAILABILITY CODES	
DISC.	AVAIL. SEC/PT. REF.
24	

Do not return this copy. Retain or destroy.

# FIELD EFFECT LIQUID CRYSTAL

J. A. Castellano  
et al

RCA Corporation

This document is subject to special  
export controls and each transmittal  
to foreign governments or foreign na-  
tionals may be made only with prior  
approval of RADC (EMBDE), GAFB,  
NY 13440.

## FOREWORD

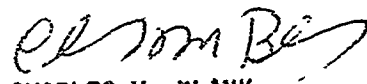
This final report was prepared by RCA Corporation, RCA Laboratories, Princeton, N. J., under Contract No. F30602-69-C-0142, Project 5597, Task 559704, covering the period 19 December 1968 to 18 December 1969.

The report covers research conducted in the Consumer Electronic Research Laboratory, D. P. McCoy, Director. C. H. Heilmeier was the Project Supervisor and J. A. Castellano was the Project Scientist. J. E. Goldmacher, W. H. Helfrich, L. A. Zaroni, R. N. Friel, M. T. McCaffrey, E. F. Pasierb, and A. Sussman also participated in the research and writing of this report. The RADC Project Engineer was Charles Blank (EMBDE).

Distribution of this document is limited under the U.S. Mutual Security Acts of 1949.

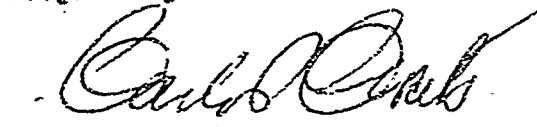
This technical report has been reviewed and is approved.

Approved:



CHARLES M. BLANK  
Project Engineer

Approved:



WILLIAM P. BETHKE  
Chief, Information Sciences Division

FOR THE COMMANDER:

  
IRVING J. GABELMAN  
Chief, Plans Office

# ABSTRACT

A new series of nematic liquid crystals based on p-alkylcarbonato-p'-alkoxyphenyl benzoates was prepared. Binary and ternary mixtures of selected derivatives taken from this series exhibited nematic behavior at or near room temperature. These materials were found to exhibit a highly efficient scattering system with a gated ac signal at 120 V. A study of the orientation pattern of domain formation and the generation of disclination loops was undertaken in an effort to further elucidate the mechanism of dynamic scattering. A practical and useful technique for the sealing and encapsulation of liquid crystal cells was developed. This procedure was applied to the fabrication of two numeric indicators and a transmission window which were furnished under the contract.

## EVALUATION

The objective of this effort was to determine the applicability of the nematic class of liquid crystal materials to Air Force display applications. The primary emphasis of this effort was improvement of the life characteristics, both through the development of new room temperature materials and through improved encapsulation and electroding techniques. In addition, some effort was directed toward developing a model of the dynamic scattering phenomena.

New room temperature materials were developed. They exhibited highly efficient light scattering, however, the voltage needed was significantly higher than that required for previously developed materials. An encapsulation technique which prevents the sealant from coming in contact with the liquid crystal material was developed and successfully applied in the fabrication of the breadboard models. Although not fully developed, progress was made in developing a model of the dynamic scattering mechanism.

Since the primary goal of obtaining long-life encapsulation was achieved, no further effort is planned in this area. The phenomena has been shown to be display compatible and one may now consider employing these materials to form the types of displays to which they are applicable. One should always bear in mind the viewing angle constraints and the necessity to carefully control the direction of the incident illumination.

  
CHARLES M. BLANK  
Project Engineer

## TABLE OF CONTENTS

Section	Page
I. INTRODUCTION . . . . .	1
II. MATERIALS. . . . .	2
A. General. . . . .	2
B. Single Nematic Compounds . . . . .	3
C. Mixed Nematic Systems. . . . .	21
III. ELECTRO-OPTICAL RESPONSE MEASUREMENTS. . . . .	28
IV. MECHANISM OF DYNAMIC SCATTERING IN NEMATIC LIQUID CRYSTALS . .	30
A. Domains. . . . .	30
B. Disclinations. . . . .	33
V. FABRICATION AND ENCAPSULATION. . . . .	36
VI. STATE-OF-THE-ART DEVICES . . . . .	40
VII. CONCLUSIONS. . . . .	45
REFERENCES. . . . .	46



## ILLUSTRATIONS

Figure	Page
1. Molecular arrangements in the liquid crystalline state . . . . .	3
2. Phase transition plot for the series: $\text{CH}_3\text{OCO}_2\text{C}_6\text{H}_4\text{CO}_2\text{C}_6\text{H}_4\text{OR}$ . . .	8
3. Phase transition plot for the series: $\text{C}_2\text{H}_5\text{OCO}_2\text{C}_6\text{H}_4\text{CO}_2\text{C}_6\text{H}_4\text{OR}$ . . .	9
4. Phase transition plot for the series: $\text{C}_3\text{H}_7\text{OCO}_2\text{C}_6\text{H}_4\text{CO}_2\text{C}_6\text{H}_4\text{OR}$ . . .	10
5. Phase transition plot for the series: $\text{C}_4\text{H}_9\text{OCO}_2\text{C}_6\text{H}_4\text{CO}_2\text{C}_6\text{H}_4\text{OR}$ . . .	11
6. Phase transition plot for the series: $\text{C}_5\text{H}_{11}\text{OCO}_2\text{C}_6\text{H}_4\text{CO}_2\text{C}_6\text{H}_4\text{OR}$ . . .	12
7. Phase transition plot for the series: $\text{C}_6\text{H}_{13}\text{OCO}_2\text{C}_6\text{H}_4\text{CO}_2\text{C}_6\text{H}_4\text{OR}$ . . .	13
8. Phase transition plot for the series: $\text{R}'\text{OCO}_2\text{C}_6\text{H}_4\text{CO}_2\text{C}_6\text{H}_4\text{OCH}_3$ . . .	14
9. Phase transition plot for the series: $\text{R}'\text{OCO}_2\text{C}_6\text{H}_4\text{CO}_2\text{C}_6\text{H}_4\text{OC}_2\text{H}_5$ . . .	15
10. Phase transition plot for the series: $\text{R}'\text{OCO}_2\text{C}_6\text{H}_4\text{CO}_2\text{C}_6\text{H}_4\text{OC}_3\text{H}_7$ . . .	16
11. Phase transition plot for the series: $\text{R}'\text{OCO}_2\text{C}_6\text{H}_4\text{CO}_2\text{C}_6\text{H}_4\text{OC}_4\text{H}_9$ . . .	17
12. Phase transition plot for the series: $\text{R}'\text{OCO}_2\text{C}_6\text{H}_4\text{CO}_2\text{C}_6\text{H}_4\text{OC}_5\text{H}_{11}$ . . .	18
13. Phase transition plot for the series: $\text{R}'\text{OCO}_2\text{C}_6\text{H}_4\text{CO}_2\text{C}_6\text{H}_4\text{OC}_6\text{H}_{13}$ . . .	19
14. Phase transition plot for the series: $\text{R}'\text{OCO}_2\text{C}_6\text{H}_4\text{CO}_2\text{C}_6\text{H}_4\text{OR}$ . . .	20
15. Phase diagram of binary mixture of nematic compound with non-mesomorphic compound . . . . .	22
16. Phase diagram of binary mixture of nematic compounds . . . . .	23
17. Structure of nematic mesophases. . . . .	24
18. Binary phase diagram of mixtures taken from the series: $\text{C}_6\text{H}_{13}\text{OCO}_2\text{C}_6\text{H}_4\text{CO}_2\text{C}_6\text{H}_4\text{OR}$ where $\text{R} = \text{C}_6\text{H}_{13}$ (A) and $\text{C}_7\text{H}_{15}$ (B) . . . . .	25
19. Ternary phase diagram of compounds <u>36</u> (A), <u>37</u> (B), and <u>38</u> (C) . . .	27
20. Incomplete domain texture of p-azoxyanisole as observed near the threshold voltage ( ~ 3 volts dc). Scratches indicating the direction of rubbing are seen in the lower part; total width of picture about 2 mm. . . . .	31

## ILLUSTRATIONS (Continued)

Figure	Page
21. Periodically distorted orientation pattern as inferred from experiments. The local alignment is indicated by orientation lines (they are tangential to unique axis). The pattern represents a cross section perpendicular to the axes of the domains . . . . .	32
22. Two contracting disclination loops, photographed a few seconds after removal of the generating electric field . . . . .	34
23. Assembled liquid crystal cell . . . . .	37
24. Scanning electron microscope studies of transparent conductive coatings (10,00X). . . . .	39
25. Two-digit transmission type liquid crystal cell . . . . .	41
26. Schematic diagram of integrated driving circuit for seven-segment numeric indicator . . . . .	42
27. Numeric indicator with components exposed . . . . .	43
28. Transmission type liquid crystal cell displaying a TV test pattern . . . . .	44

## SECTION I

### INTRODUCTION

The two main classes of electro-optic effects discovered to date are of the light-emitting and light-modifying type. The cathode ray tube as well as electroluminescent and gas-discharge devices are examples of light-emitting effects which have received a great deal of attention in recent years. The kinescope requires high voltages to produce the electron beam while electroluminescent and gas-discharge devices are limited in varying degrees by spectral response, brightness, life, and nature of the electrical drive.

Examples of light-modifying effects are mechanical shutters, saturable absorbers, Stark-effect or Franz-effect modulators, and effects based on field-induced changes of the index of refraction of a material (Pockels effect and Kerr effect). Mechanical shutters are likely to be limited by their speed of response and drive requirements while saturable absorbers require intense optical radiation for operation. In general, the Stark and Franz effects require extremely high fields and voltages to produce minimal shifts in absorption spectra. In addition, single-crystal materials are needed for optimum performance. The linear electro-optic effect (or Pockels effect) also requires high voltages and fields in addition to strain-free single crystals lacking inversion symmetry. The Kerr effect snares the high-voltage requirements of the linear electro-optic effect.

This report is a detailed account of our efforts to further investigate the nature and scope of a newly discovered[1] electro-optic effect of the light-modifying type which we call *dynamic scattering*. Although the mechanism of this effect has not been completely elucidated, the scattering is believed to be due to the disruptive effects of ions in transit through the ordered structure of certain classes of nematic liquid crystals. Since microscopic examination of the electrically activated liquid reveals a turbulent condition, the scattering is said to be dynamic.

The major objectives of the present investigation were the development of: (1) new room-temperature nematic systems which exhibit dynamic scattering, (2) a model for the mechanism of the dynamic scattering mode, and (3) encapsulation techniques which provide long life of the display devices based on dynamic scattering. These developments were successfully carried out under the contract, and the results were applied to the fabrication of prototype numeric indicators which operate at low voltage and over a wide range of temperatures and ambient light conditions (from complete darkness to direct sunlight). Devices of this type are expected to be useful for cockpit and computer readout displays.

## SECTION II

### MATERIALS

#### A. GENERAL

Since the field of liquid crystals has been the subject of several review articles[2,3] a comprehensive discussion will not be attempted here. However, a brief discussion of some general principles will hopefully facilitate a better understanding of the effects involved.

"Liquid crystals" are organic materials that have the mechanical properties of liquids but possess the optical properties of crystalline solids. The liquid crystalline or *mesomorphic state* is exhibited over a specific temperature range. Thus, the crystalline solid will be converted to the mesomorphic state at the *crystal-mesomorphic* transition temperature and to the normal isotropic liquid at the *mesomorphic-isotropic* transition temperature. Both of these transition temperatures are characteristic of specific compounds, and since they are thermodynamically reversible, they can be observed either upon heating or cooling the materials.

Liquid crystals are by no means rare and approximately one out of every 200 organic compounds exhibits mesomorphic behavior. Three main types of mesomorphic states have been recognized; they have been designated as the *smectic*, *cholesteric* and *nematic* mesophase. The smectic mesophase is stratified, with the molecules arranged in layers, their long axes parallel to each other in the layers and approximately normal to the plane of the layers. The layer thickness is about the length of the molecule or 20 Å. The molecules can move in two directions in the plane and they can rotate about one axis. Within the layers, they can be arranged either in neat rows (Figure 1) or randomly distributed. The planes can slide, without hindrance, over similar neighboring layers.

The cholesteric mesophase is found primarily in derivatives of cholesterol, especially the esters. The microscopic structure consists of parallel layers about 2000 Å thick. The direction of the long axis of a molecule in a chosen layer is slightly displaced from the direction of the axis in adjacent layers and produces a helical design (Figure 1). The material changes color as a function of small fluctuations in temperature as a result of changes in the pitch of this helix.

The term "nematic" is derived from the Greek word meaning thread since it describes the thread-like lines which these materials exhibit under a microscope. A sample of nematic material contained in a vial appears as a viscous, turbid, off-white liquid. The molecules of a nematic compound are arranged with their long axes parallel. In contrast to smectic materials, however, the molecules are not arranged in layers and are free to slide past each other (Figure 1). This arrangement permits nematic molecules to be oriented by electric and magnetic fields. This orientational effect makes the nematic state the most attractive mesophase for study under electric field.

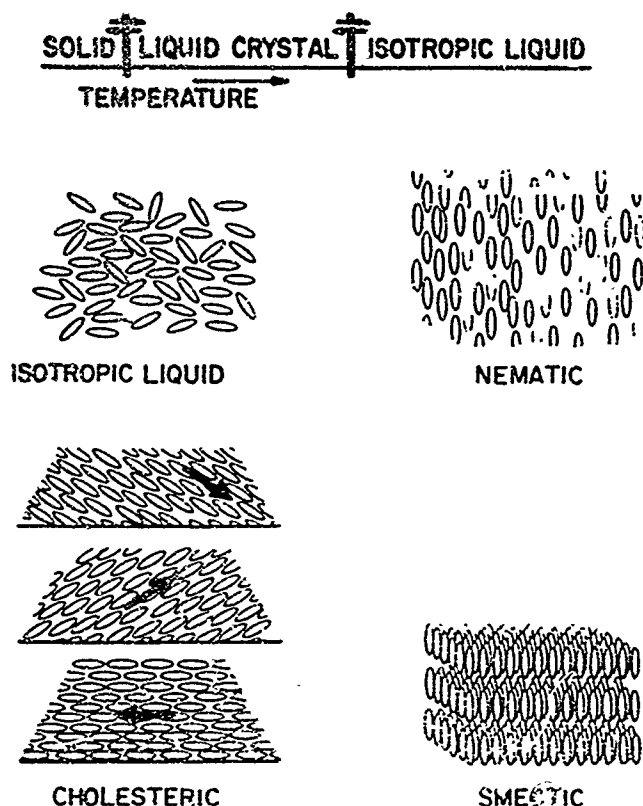


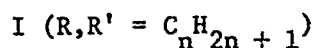
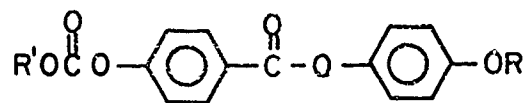
Figure 1. Molecular arrangements in the liquid crystalline state.

#### B. SINGLE NEMATIC COMPOUNDS

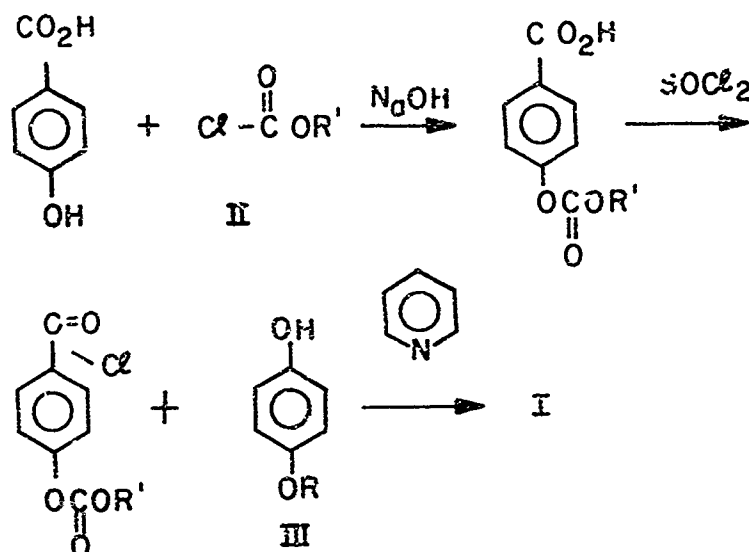
Although a large number of nematic materials have previously been prepared, very few known compounds exhibit crystal-nematic transition temperatures at or below room temperature. In the past most workers were concerned with the synthesis of compounds with high nematic thermal stability (a high nematic-isotropic transition temperature), and as a result of the relatively high molecular weight of the compounds which they prepared, high crystal-nematic transition temperatures were obtained. Our efforts during the past several years have, therefore, been directed toward the preparation of comparatively low molecular weight materials[4,5]. This work led to the development of materials which exhibited nematic behavior at room temperature. The research reported under this contract was directed toward the preparation of room-temperature nematic systems which differed from those previously reported.

Molecules that exhibit nematic mesomorphism are generally cylindrically shaped and possess polar and/or polarizable groups in addition to aromatic

rings. The compounds selected for study possessed these characteristics as they were derived from p-alkylcarbonato-p'-alkoxyphenyl benzoates (I)



The compounds were prepared in three steps by the following synthetic route:



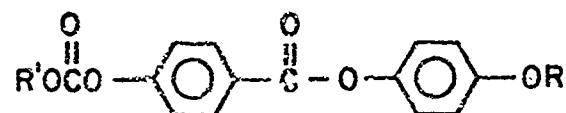
Both the alkyl chloroformates[6] (II) and alkoxyphenols[6] (III) contained from one to seven carbon atoms in a straight chain\*. The products, which were obtained in 40 to 60% overall yield, were purified by repeated recrystallizations from hexane. Recrystallization was continued until the nematic-isotropic transition temperature was constant and reversible[7]. This resulted in materials with resistivities of  $10^9$  to  $10^{10}$  ohm-cm. The compounds were then characterized by elemental analysis[8]. The transition temperatures were measured in open capillary tubes with an Arthur H. Thomas Unimelt apparatus[9]. The results of this work are presented in Table I.

Of the 48 compounds that were prepared 27 exhibited enantiotropic behavior (melting point *below* nematic-isotropic transition), 14 were monotropic (melting point *above* nematic-isotropic transition) and only seven were non-nematic. Since the supercooled nematic mesophase (monotropic state) may crystallize at any time, compounds which exhibit this type of behavior are not suitable for the construction of electro-optic cells. Thus, we must consider only the 27 enantiotropic compounds useful for study under electrical excitation.

\*In several cases the alkoxy chain contained eight carbon atoms.

TABLE I

p-Alkylcarbonato-p'-Alkoxyphenyl Benzoates



No.	R	R'	Crystal-Nematic Transition °C	Nematic-Isotropic Transition °C
1	CH <sub>3</sub>	CH <sub>3</sub>	--	115 <sup>a</sup>
2	C <sub>2</sub> H <sub>5</sub>	CH <sub>3</sub>	86	110
3	C <sub>3</sub> H <sub>7</sub>	CH <sub>3</sub>	--	106 (83) <sup>b</sup>
4	C <sub>4</sub> H <sub>9</sub>	CH <sub>3</sub>	91	96
5	C <sub>5</sub> H <sub>11</sub>	CH <sub>3</sub>	--	109 (85) <sup>b</sup>
6	C <sub>6</sub> H <sub>13</sub>	CH <sub>3</sub>	--	75 <sup>a</sup>
7	C <sub>7</sub> H <sub>15</sub>	CH <sub>3</sub>	52	66
8	C <sub>8</sub> H <sub>17</sub>	CH <sub>3</sub>	--	80 <sup>a</sup>
9	CH <sub>3</sub>	C <sub>2</sub> H <sub>5</sub>	--	110 (82) <sup>b</sup>
10	C <sub>2</sub> H <sub>5</sub>	C <sub>2</sub> H <sub>5</sub>	--	104 (96) <sup>b</sup>
11	C <sub>3</sub> H <sub>7</sub>	C <sub>2</sub> H <sub>5</sub>	--	86 <sup>a</sup>
12	C <sub>4</sub> H <sub>9</sub>	C <sub>2</sub> H <sub>5</sub>	--	98 (80) <sup>b</sup>
13	C <sub>5</sub> H <sub>11</sub>	C <sub>2</sub> H <sub>5</sub>	--	81 (78) <sup>b</sup>
14	C <sub>6</sub> H <sub>13</sub>	C <sub>2</sub> H <sub>5</sub>	75	91
15	C <sub>7</sub> H <sub>15</sub>	C <sub>2</sub> H <sub>5</sub>	70	83
16	CH <sub>3</sub>	C <sub>3</sub> H <sub>7</sub>	--	78 (60) <sup>b</sup>
17	C <sub>2</sub> H <sub>5</sub>	C <sub>3</sub> H <sub>7</sub>	--	82 (79) <sup>b</sup>
18	C <sub>3</sub> H <sub>7</sub>	C <sub>3</sub> H <sub>7</sub>	--	76 <sup>a</sup>
19	C <sub>4</sub> H <sub>9</sub>	C <sub>3</sub> H <sub>7</sub>	--	84 (71) <sup>b</sup>
20	C <sub>5</sub> H <sub>11</sub>	C <sub>3</sub> H <sub>7</sub>	--	71 (65) <sup>b</sup>
21	C <sub>6</sub> H <sub>13</sub>	C <sub>3</sub> H <sub>7</sub>	70	73
22	C <sub>7</sub> H <sub>15</sub>	C <sub>3</sub> H <sub>7</sub>	58	68
23	C <sub>8</sub> H <sub>17</sub>	C <sub>3</sub> H <sub>7</sub>	--	48 <sup>a</sup>
24	CH <sub>3</sub>	C <sub>4</sub> H <sub>9</sub>	--	70 (57) <sup>b</sup>

(a) Not nematic; (b) Monotropic.

TABLE I (Continued)

No.	R	R'	Crystal-Nematic Transition °C	Nematic-Isotropic Transition °C
25	C <sub>2</sub> H <sub>5</sub>	C <sub>4</sub> H <sub>9</sub>	49	90
26	C <sub>3</sub> H <sub>7</sub>	C <sub>4</sub> H <sub>9</sub>	--	70 (67) <sup>b</sup>
27	C <sub>4</sub> H <sub>9</sub>	C <sub>4</sub> H <sub>9</sub>	74	81
28	C <sub>5</sub> H <sub>11</sub>	C <sub>4</sub> H <sub>9</sub>	53	69
29	C <sub>6</sub> H <sub>13</sub>	C <sub>4</sub> H <sub>9</sub>	44	84
30	C <sub>7</sub> H <sub>15</sub>	C <sub>4</sub> H <sub>9</sub>	45	74
31	C <sub>8</sub> H <sub>17</sub>	C <sub>4</sub> H <sub>9</sub>	--	77 <sup>a</sup>
32	CH <sub>3</sub>	C <sub>5</sub> H <sub>11</sub>	--	54 (53) <sup>b</sup>
33	C <sub>2</sub> H <sub>5</sub>	C <sub>5</sub> H <sub>11</sub>	59	74
34	C <sub>3</sub> H <sub>7</sub>	C <sub>5</sub> H <sub>11</sub>	67	72
35	C <sub>4</sub> H <sub>9</sub>	C <sub>5</sub> H <sub>11</sub>	53	74
36	C <sub>5</sub> H <sub>11</sub>	C <sub>5</sub> H <sub>11</sub>	45	85
37	C <sub>6</sub> H <sub>13</sub>	C <sub>5</sub> H <sub>11</sub>	42	76
38	C <sub>7</sub> H <sub>15</sub>	C <sub>5</sub> H <sub>11</sub>	47	72
39	CH <sub>3</sub>	C <sub>6</sub> H <sub>13</sub>	--	57 (56) <sup>b</sup>
40	C <sub>2</sub> H <sub>5</sub>	C <sub>6</sub> H <sub>13</sub>	64	79
41	C <sub>3</sub> H <sub>7</sub>	C <sub>6</sub> H <sub>13</sub>	71	86
42	C <sub>4</sub> H <sub>9</sub>	C <sub>6</sub> H <sub>13</sub>	48	80
43	C <sub>5</sub> H <sub>11</sub>	C <sub>6</sub> H <sub>13</sub>	41	89
44	C <sub>6</sub> H <sub>13</sub>	C <sub>6</sub> H <sub>13</sub>	43	84
45	C <sub>7</sub> H <sub>15</sub>	C <sub>6</sub> H <sub>13</sub>	36	54
46	CH <sub>3</sub>	C <sub>7</sub> H <sub>15</sub>	55	81
47	C <sub>2</sub> H <sub>5</sub>	C <sub>7</sub> H <sub>15</sub>	60	91
48	C <sub>3</sub> H <sub>7</sub>	C <sub>7</sub> H <sub>15</sub>	58	91

(a) Not nematic; (b) Monotropic.



In order to facilitate a better understanding of the effects of changes in molecular structure as a function of mesomorphic behavior, the data of Table I have been used to construct a series of phase transition plots. These diagrams (Figures 2 through 13) illustrate the changes in phase transition temperatures with an increase in the length of an alkyl chain attached to a terminal position of the molecule. It is well known[2] that when the nematic-isotropic transition temperature for a homologous series of compounds, e.g., in a series of *n*-alkyl ethers or esters, is plotted against the number of carbon atoms in the alkyl chain, a regular alternation of the nematic-isotropic transition temperatures occurs. This behavior, which was found to occur with all of the series reported here, has been explained by assuming that the alkyl chains adopt the "cog wheel" rather than the "zig zag" conformation in the mesomorphic state[2].

Another well-known phenomenon which occurs with liquid crystals as well as with some other organic compounds is a decrease in the melting points of derivatives of a homologous series of compounds with an increase in the length of an alkyl chain. Since the melting characteristics of a compound are largely determined by the strength of intermolecular interactions in the crystal lattice, it follows that a reduction in the strength of these interactions by separation of the active centers of charge would produce lower melting materials. Thus, as we increase the length of an alkyl chain the dipolar (alkoxy) and polarizable (azomethane) centers of the molecule become further separated from one another, and lower melting points are produced.

In the first series of derivatives (Figure 2) the methyl carbonato group produces such strong terminal intermolecular attractions that extension of the chain in the alkoxy portion (OR) does not produce a dramatic reduction in melting point until the chain contains seven carbon atoms. However, as we proceeded to increase the chain in the carbonato ester portion of the molecule these terminal interactions were reduced. Thus, compounds which contain from four to six carbon atoms in the carbonato chain gave a lower melting series of derivatives and as a result a larger number of enantiotropic compounds (Figures 5, 6, and 7). Similar results were obtained when the alkoxy chain was kept constant and the carbonato chain was extended as illustrated in Figures 8 through 13. A summary of this effect is presented in Figure 14 which illustrates a dramatic reduction in melting point when both chains are increased simultaneously. This plot also shows a systematic increase in nematic thermal stability with increasing chain length.

The above results might lead to the conclusion that a further increase in the lengths of both the carbonato ester and alkoxy chain would produce compounds with lower melting points and even wider nematic changes. Past experience, however, has shown that chain lengths of eight or more carbon atoms produce such weak terminal interactions that the critical balance of lateral to terminal attractive forces is upset, and the lateral interactions become important. An increase in the ratio of lateral to terminal cohesions always results in the appearance of smectic behavior (the smectic mesophase does not respond to low voltage electric fields). Further increases in the chain length then result in increased smectic thermal stability and shorter nematic ranges. In order to produce materials with lower melting points and wide nematic ranges, it was therefore necessary to use a mixture of nematic compounds.

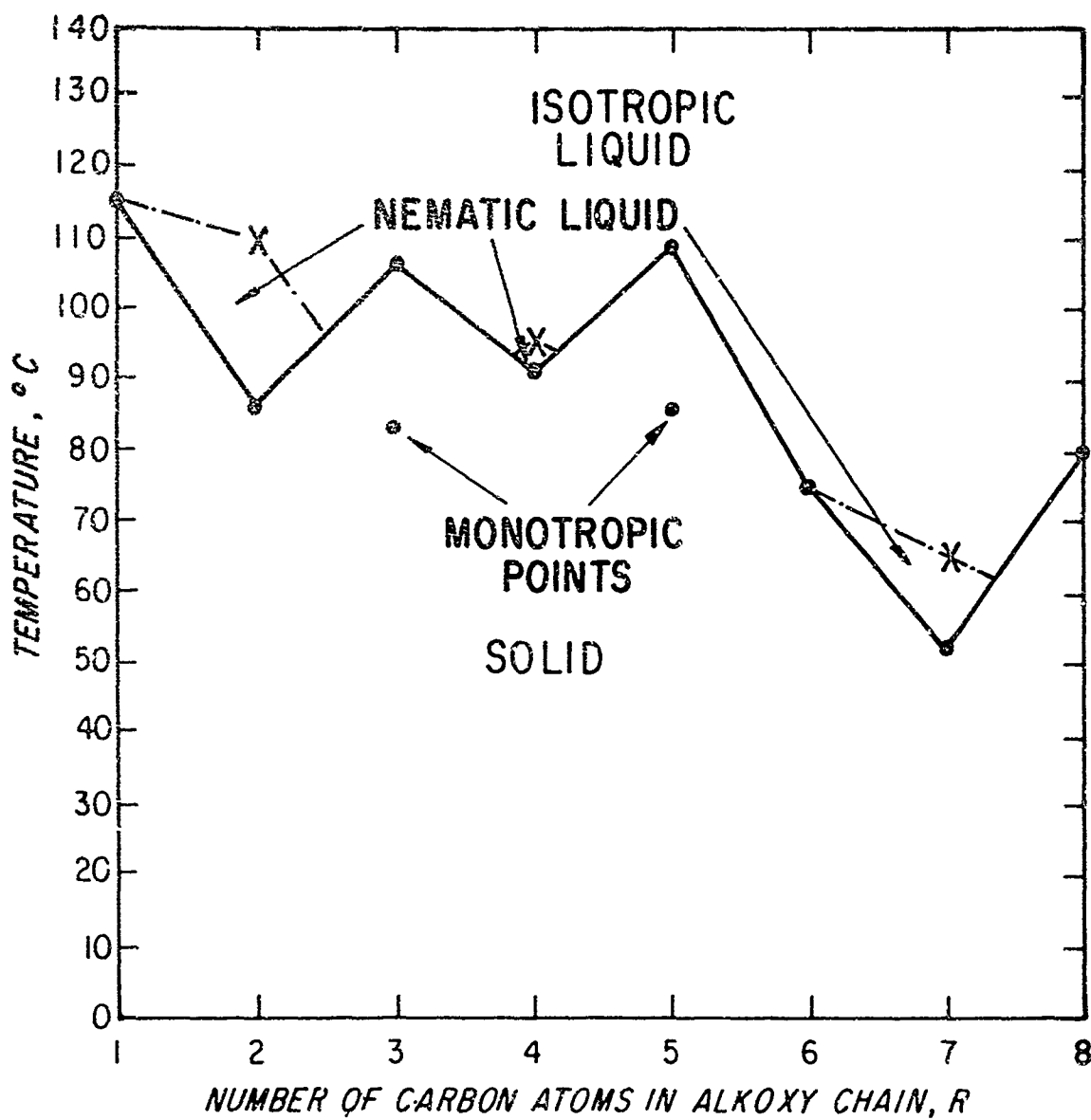


Figure 2. Phase transition plot for the series:  
 $\text{CH}_3\text{OCO}_2\text{C}_6\text{H}_4\text{CO}_2\text{C}_6\text{H}_4\text{OR}$ .

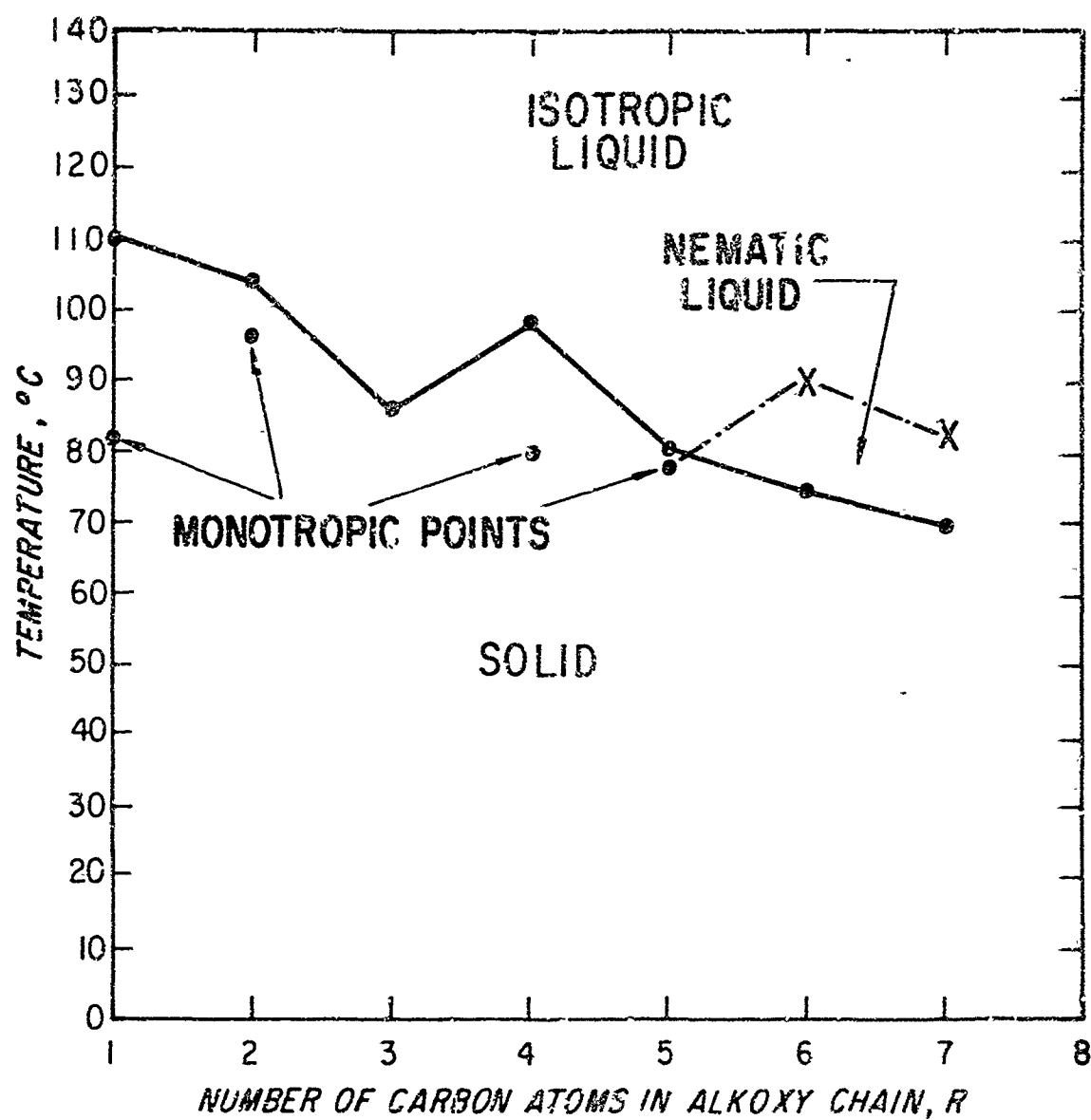


Figure 3. Phase transition plot for the series:  
 $C_{25}H_{50}O_2C_6H_4CO_2C_6H_4OR.$

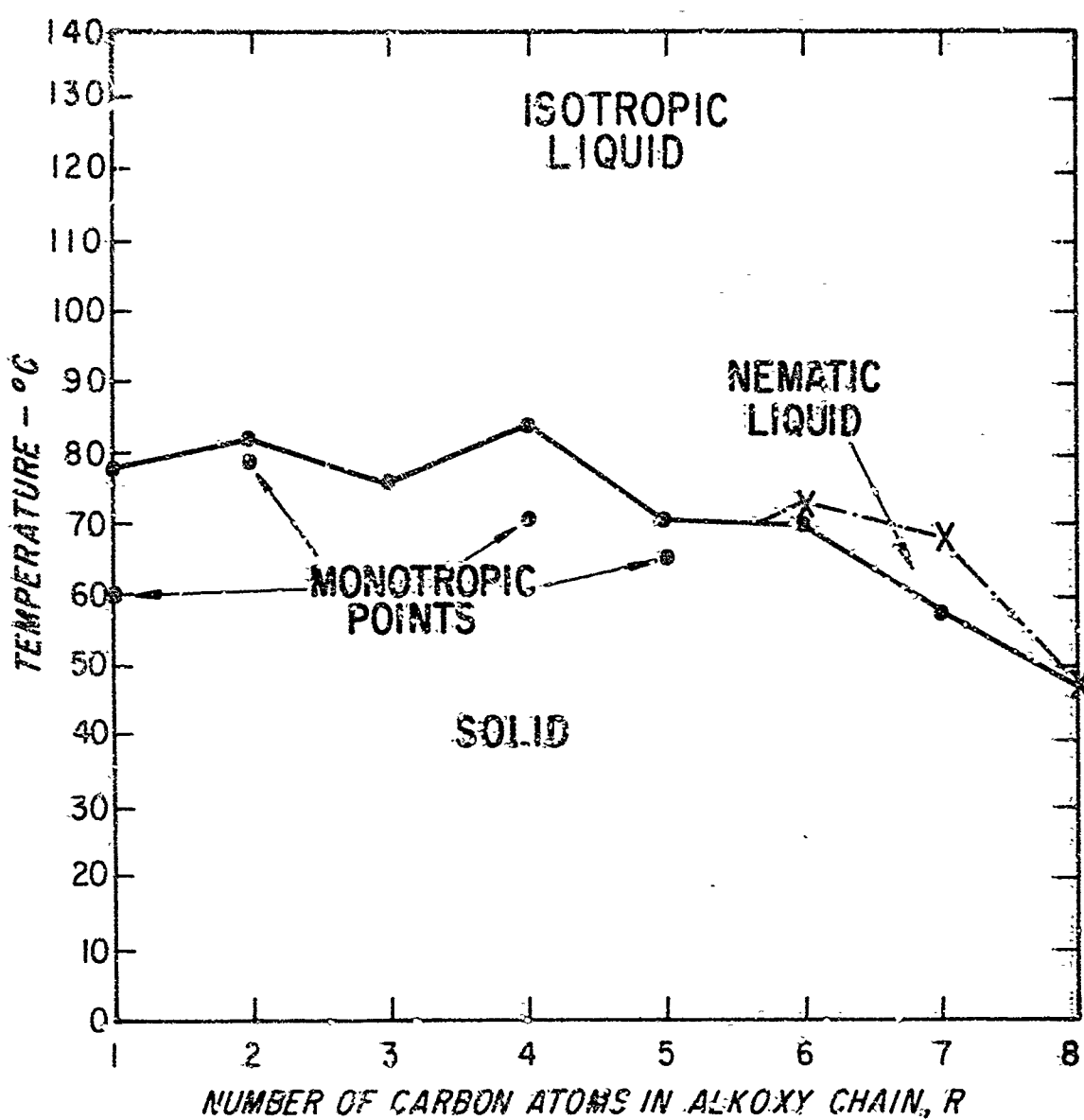


Figure 4. Phase transition plot for the series:  
 $C_3H_7OCO_2C_6H_4CO_2C_6H_4OR.$

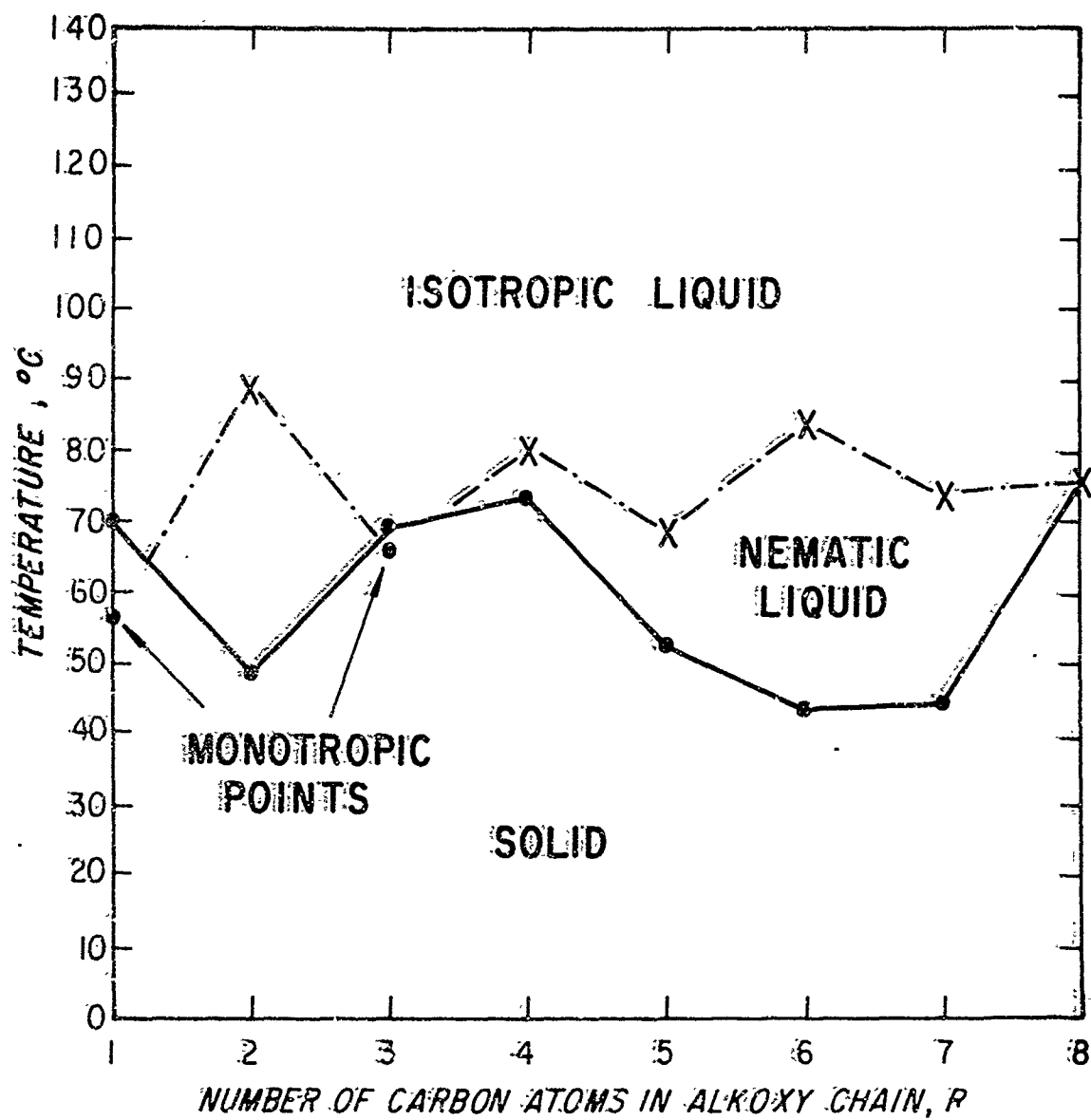


Figure 5. Phase transition plot for the series:  
 $C_4H_9OCO_2C_6H_4CO_2C_6H_4OR$ .

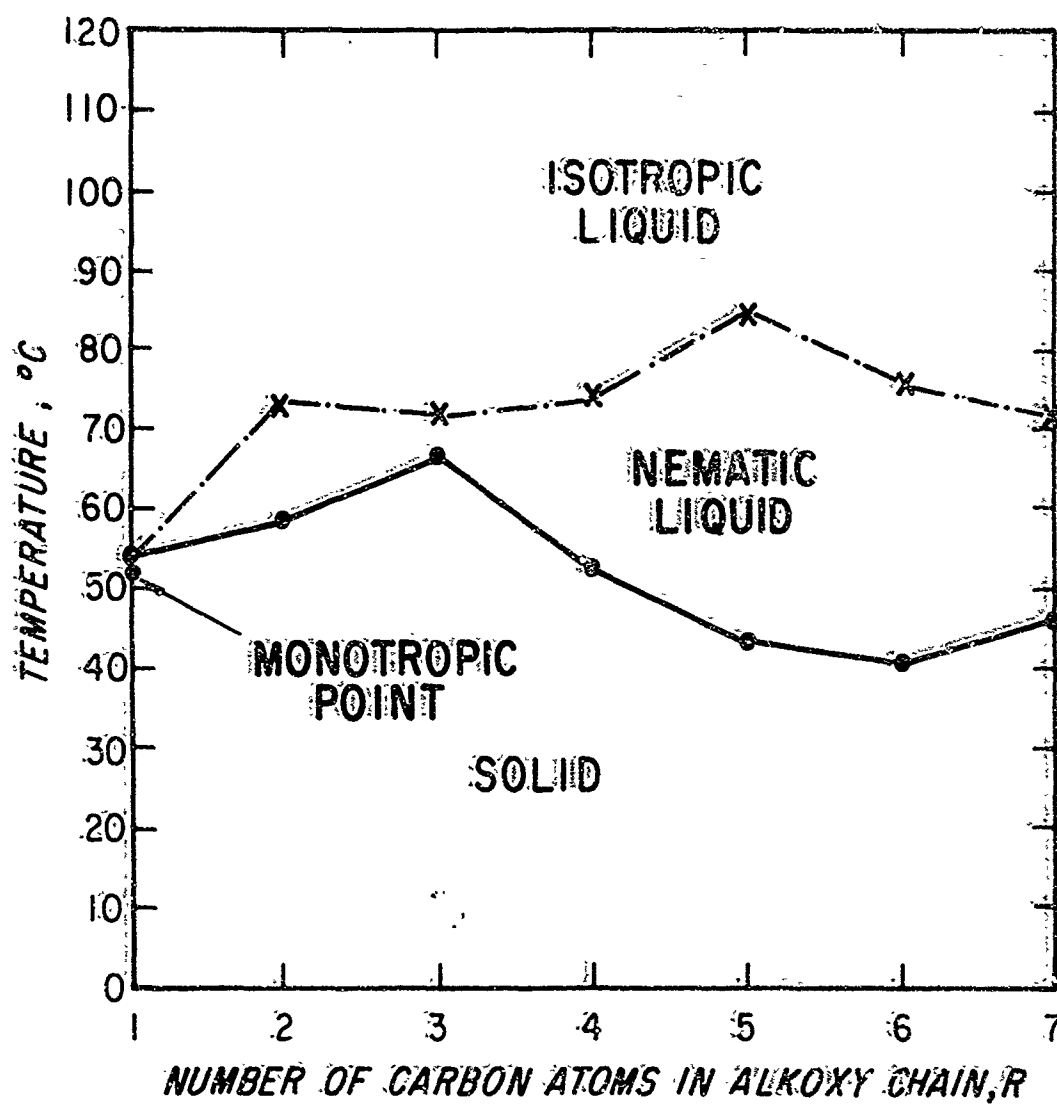


Figure 6. Phase transition plot for the series:  
 $C_5H_{11}OCO_2C_6H_4CO_2C_6H_4OR$ .

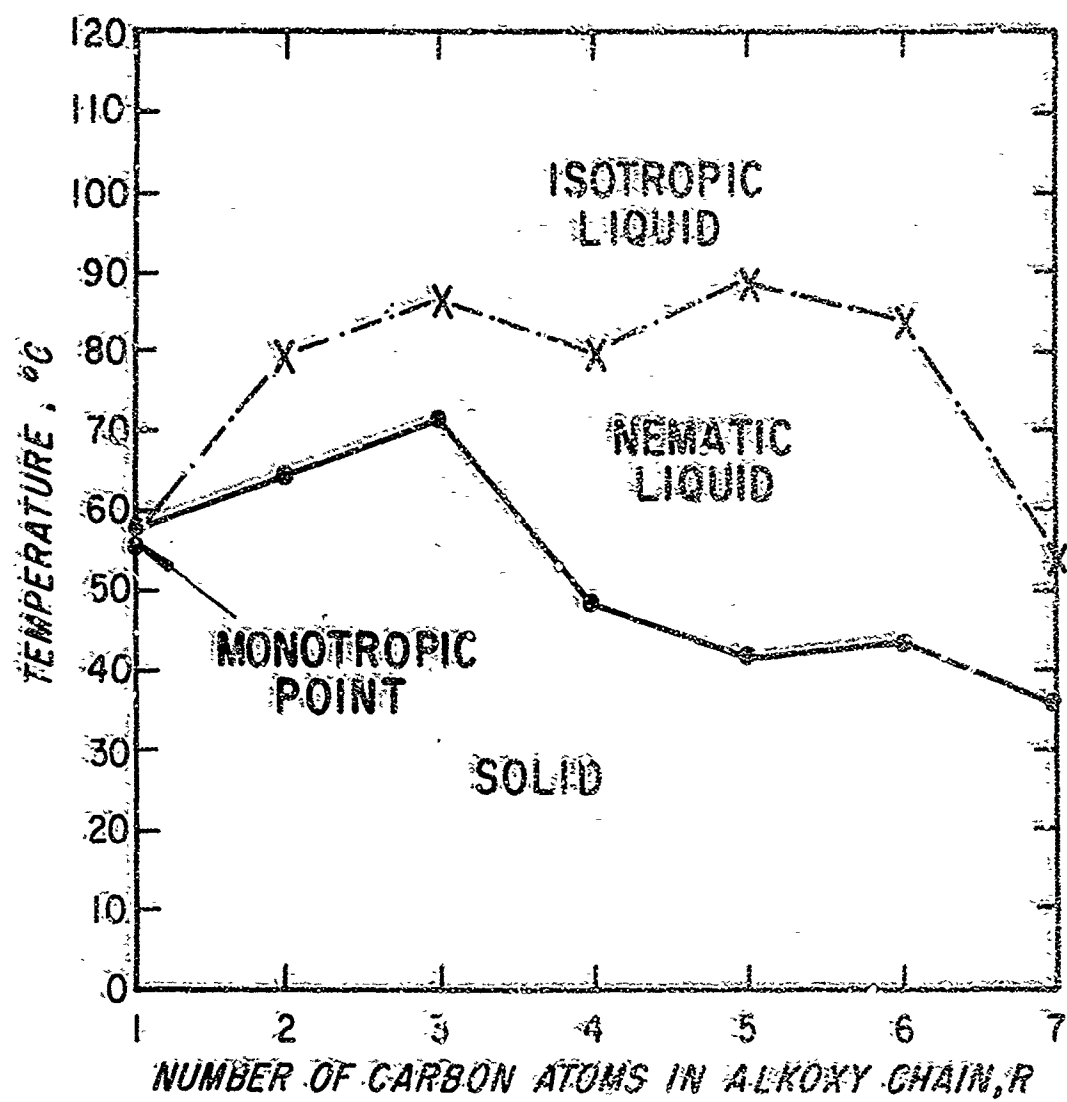


Figure 7. Phase transition plot for the series:  
 $C_6H_{13}CO_2C_6H_4CO_2C_6H_4OR$ .

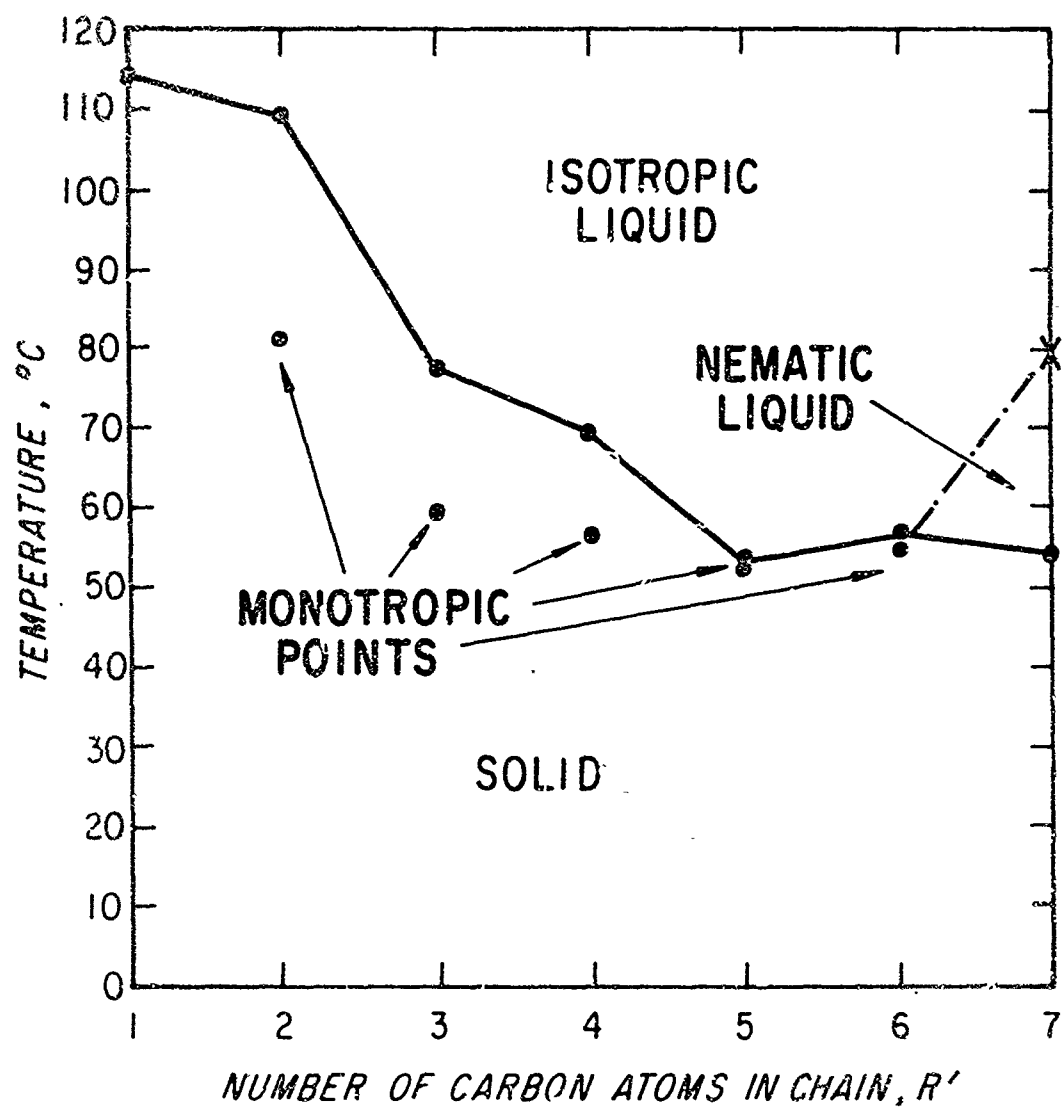


Figure 8. Phase transition plot for the series:  
 $R'OCO_2C_6H_4CO_2C_6H_4OCH_3$ .



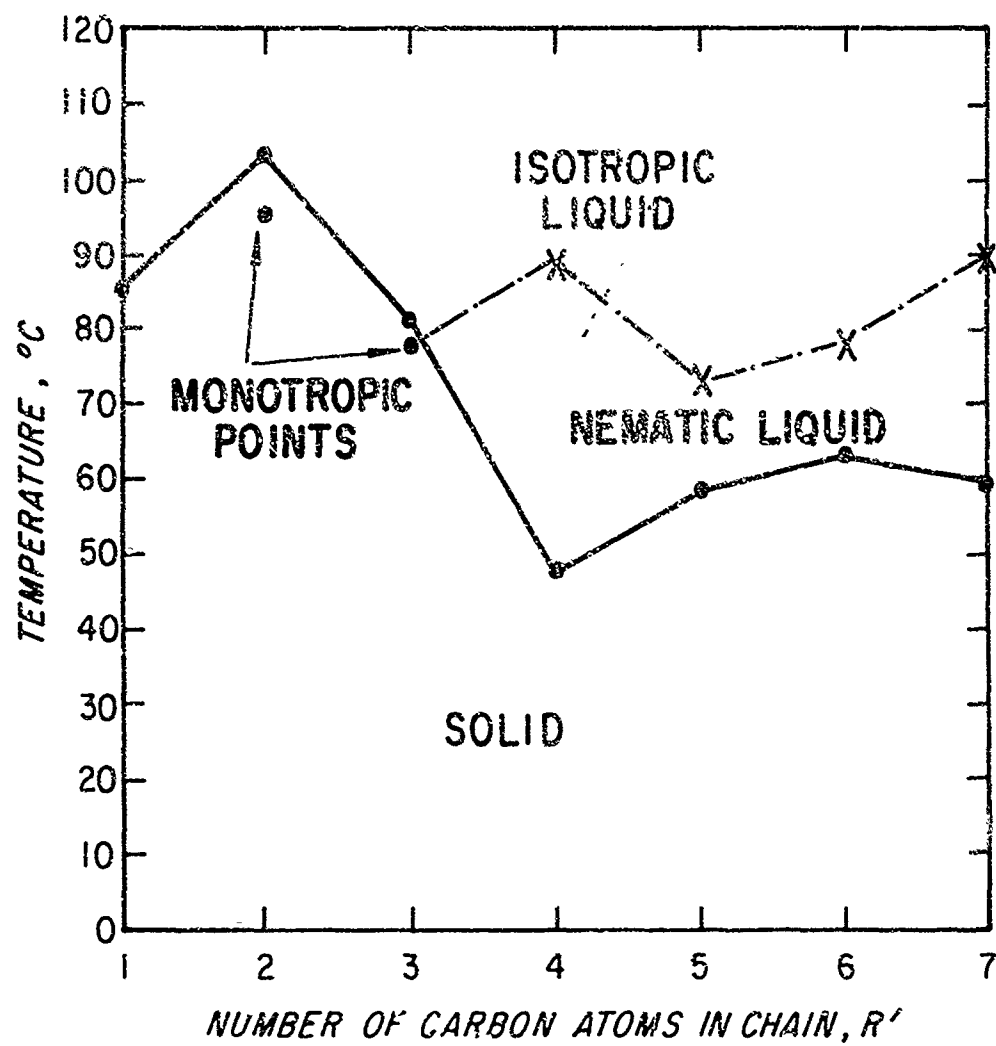


Figure 9. Phase transition plot for the series:  
 $R'OCO_2C_6H_4CO_2C_6H_4OC_2H_5$ .

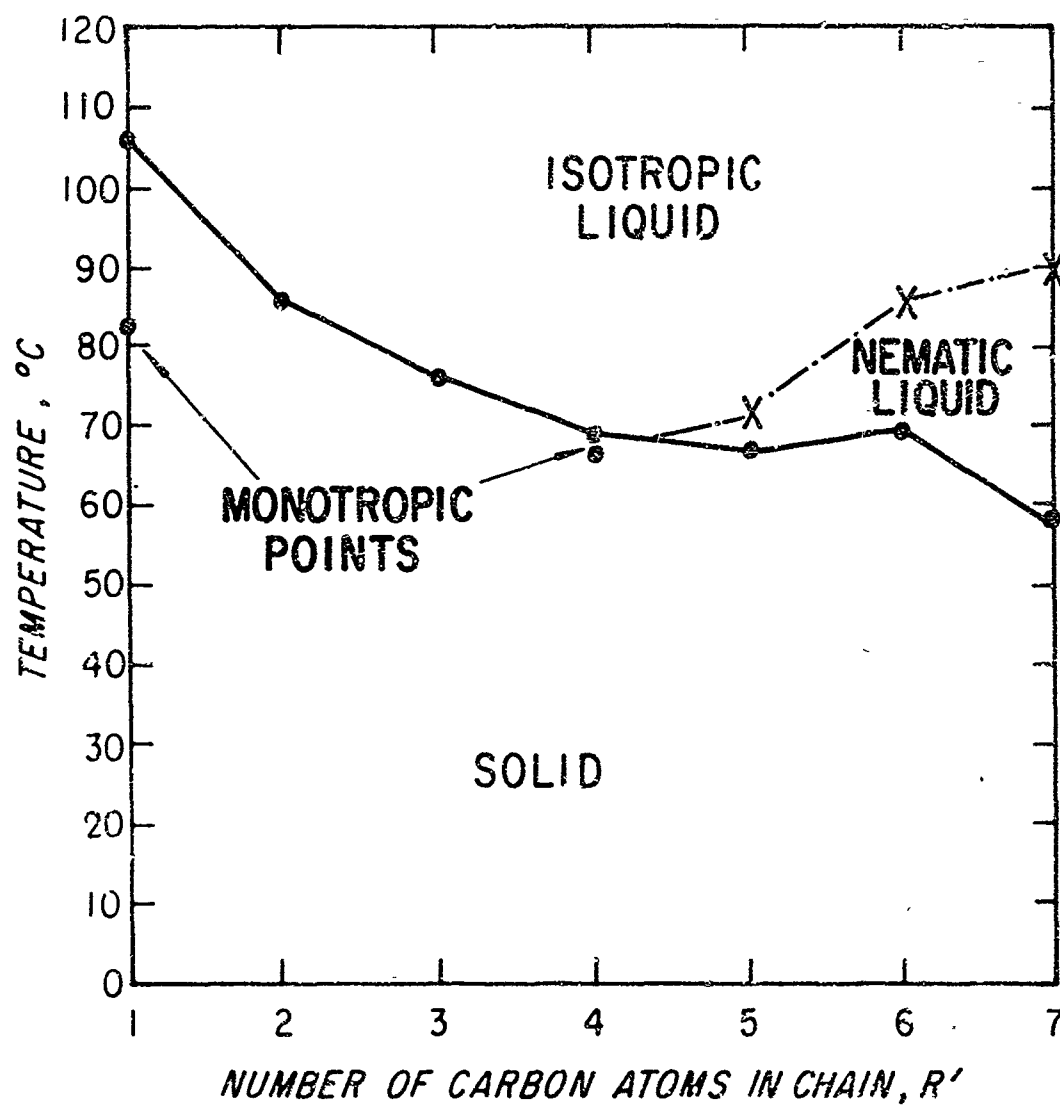


Figure 10. Phase transition plot for the series:  
 $R'OCO_2C_6H_4CO_2C_6H_4OC_3H_7$ .

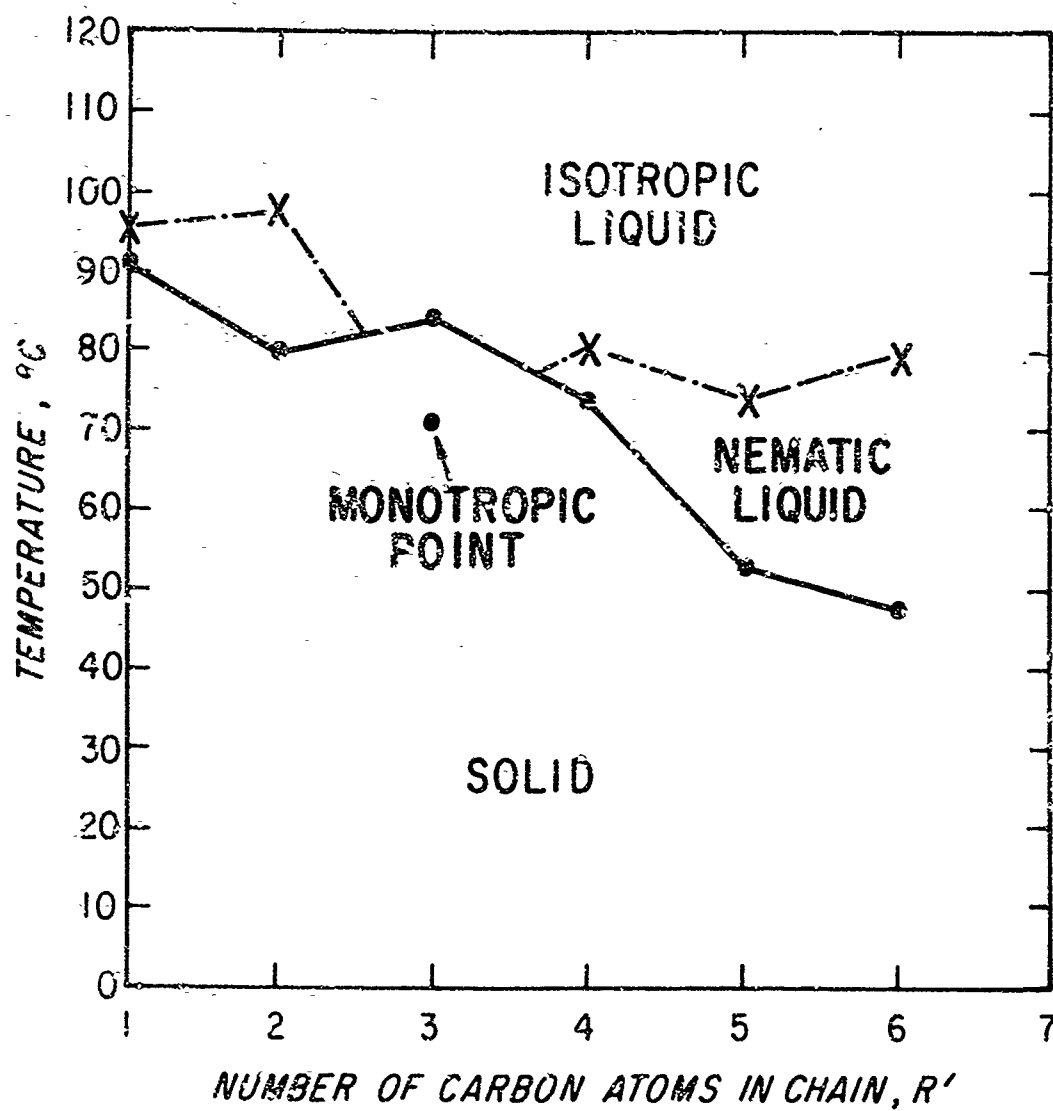


Figure 11. Phase transition plot for the series:  
 $R'OCO_2C_6H_4CO_2C_6H_4OC_4H_9$ .

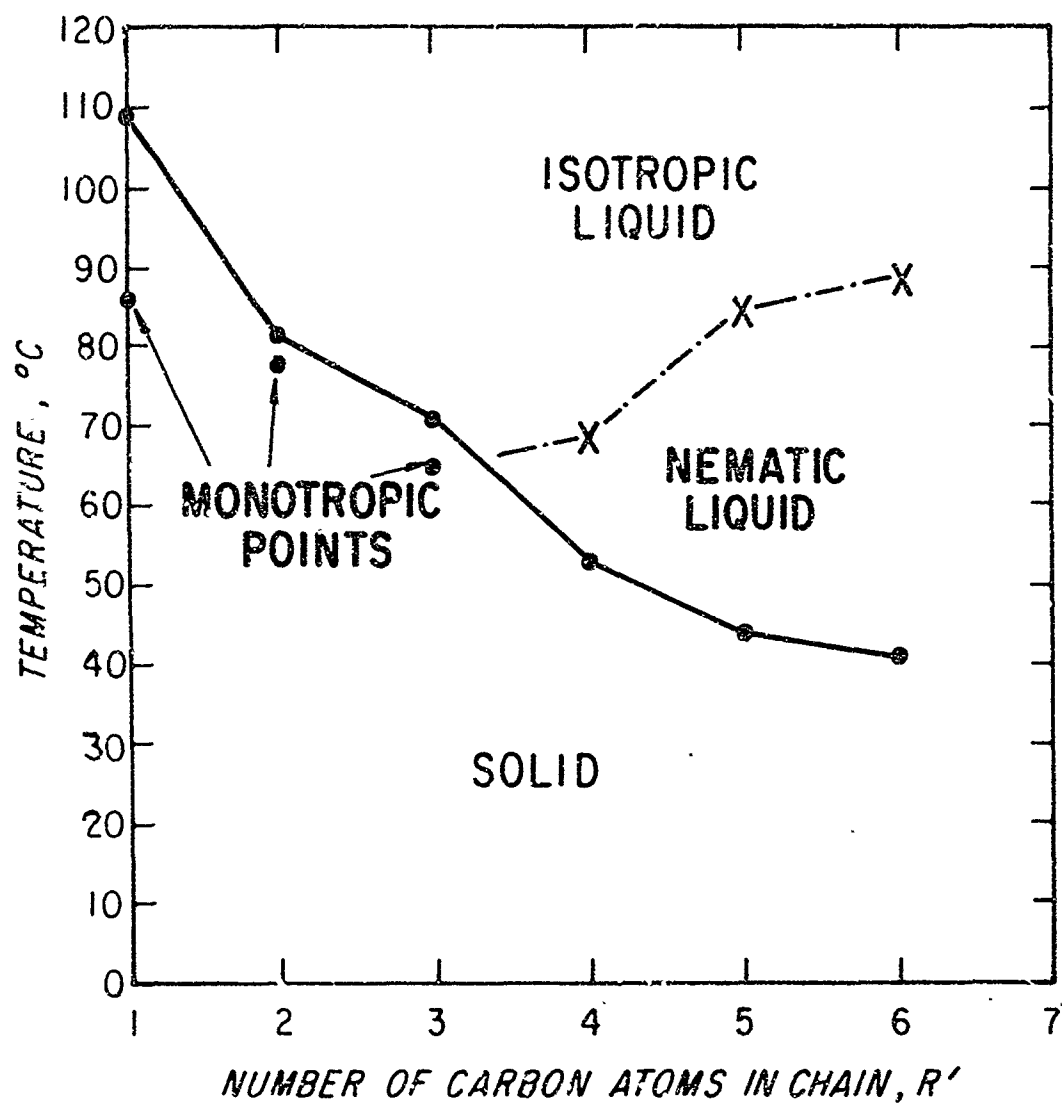


Figure 12. Phase transition plot for the series:  
 $R'OC\dot{O}_2C_6H_4CO_2C_6H_4OC_5H_{11}$ .

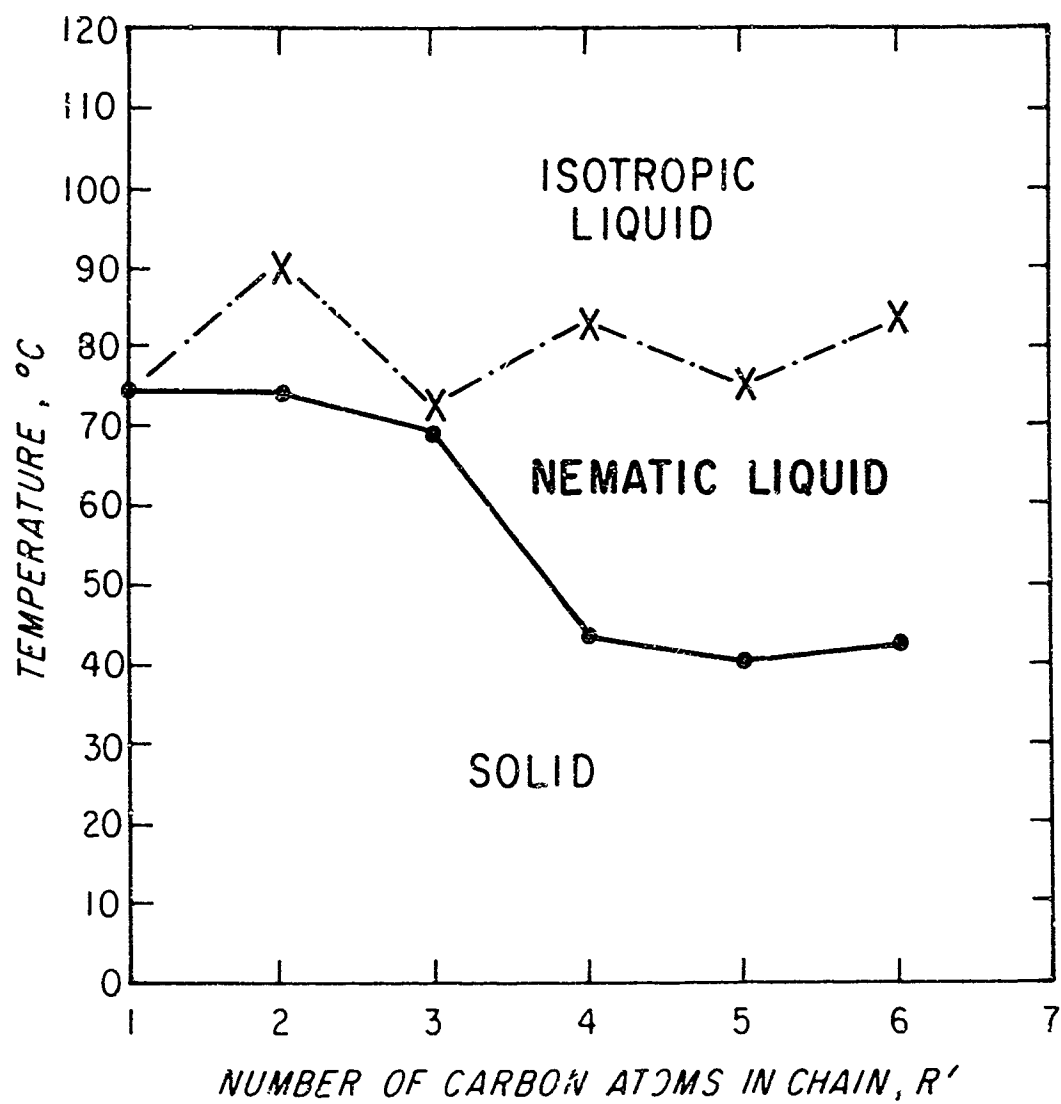


Figure 13. Phase transition plot for the series:  
 $R'OCO_2C_6H_4CO_2C_6H_4OC_6H_{13}$ .

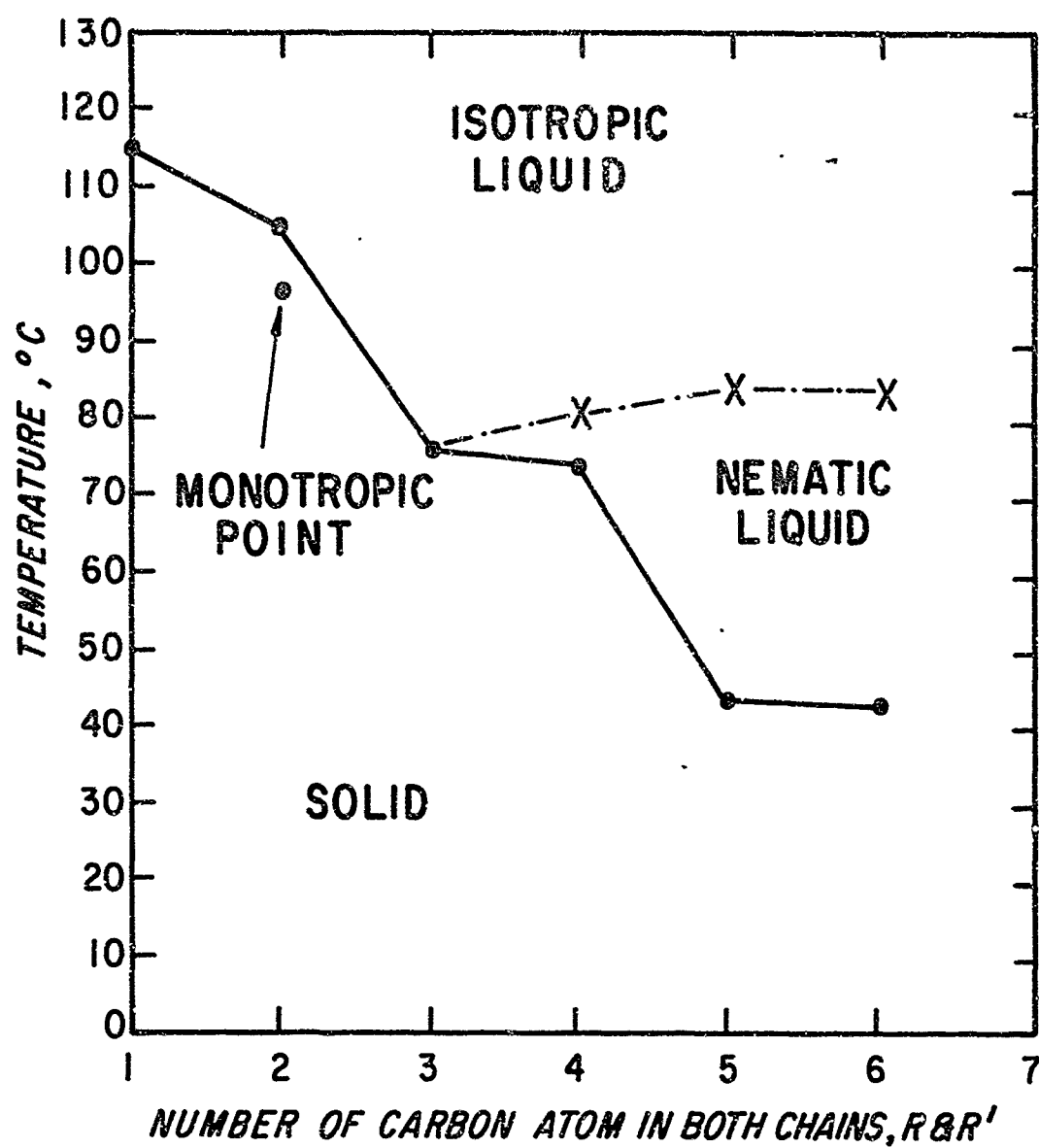


Figure 14. Phase transition plot for the series:  
 $R'OCO_2C_6H_4CO_2C_6H_4OR$ .

### C. MIXED NEMATIC SYSTEMS

Mixtures of linear, non-mesomorphic molecules with nematic compounds have been investigated previously. These systems are always characterized by a sharp decrease in both the nematic  $\rightarrow$  liquid and crystal  $\rightarrow$  nematic transition temperature with increasing concentration of non-mesomorphic component. An example of this type of system has recently been reported[10] with mixtures of *p*-azoxyanisole (nematic) and *p*'-chloraniline (non-mesomorphic). The phase diagram for this binary mixture is illustrated in Figure 15.

Mixtures of two or more nematic compounds which possess subtle differences in molecular structure do not exhibit decreases in their nematic  $\rightarrow$  liquid transition temperatures with molar composition although eutectic points for the crystal  $\rightarrow$  nematic transition temperatures are obtained. An example of this phenomenon was first reported by Demus[11]; a phase diagram for the binary system which he used is illustrated in Figure 16. Thus, the nematic  $\rightarrow$  isotropic liquid transition temperatures form a smooth curve over the entire range of molar composition.

These effects can be explained by the following model: The molecules of a non-mesomorphic guest are randomly oriented in a nematic host, and the presence of small quantities is sufficient to cause disruption of nematic order. This is illustrated in Figure 17(b) where the dark ovals represent the non-nematic guest. On the other hand, mixtures of nematic compounds with almost identical structures have stable mesophases at all molar compositions because all the molecules are oriented in the same direction. This results in the formation of a "nematic lattice" as shown in Figure 17(c).

These concepts were successfully applied to binary and ternary mixtures of several carbonate derivatives of Table I. Thus, a series of binary mixtures of compounds 44 and 45 was prepared and the transition temperatures measured. The results are presented in Table II and Figure 18.

The eutectic mixture (40% A, 60% B) had a crystal  $\rightarrow$  nematic transition temperature at 27°C and a nematic isotropic transition at 73°C. It was possible to obtain materials with even lower crystal  $\rightarrow$  nematic transition temperatures by preparing ternary mixtures containing compounds 36, 37, and 38. These results are shown in Table III and a ternary phase diagram is presented in Figure 19. The eutectic mixture (20% A, 40% B, and 40% C) had a crystal  $\rightarrow$  nematic transition temperature at 24°C and a nematic  $\rightarrow$  isotropic transition at 76°C. In addition, seven other mixtures which had crystal  $\rightarrow$  nematic transition temperatures below 30°C were prepared by this technique.

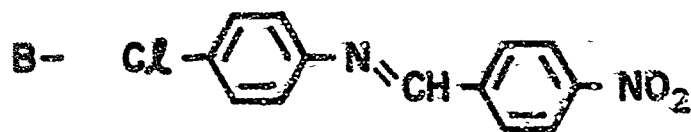
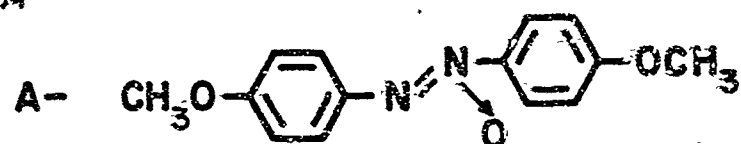
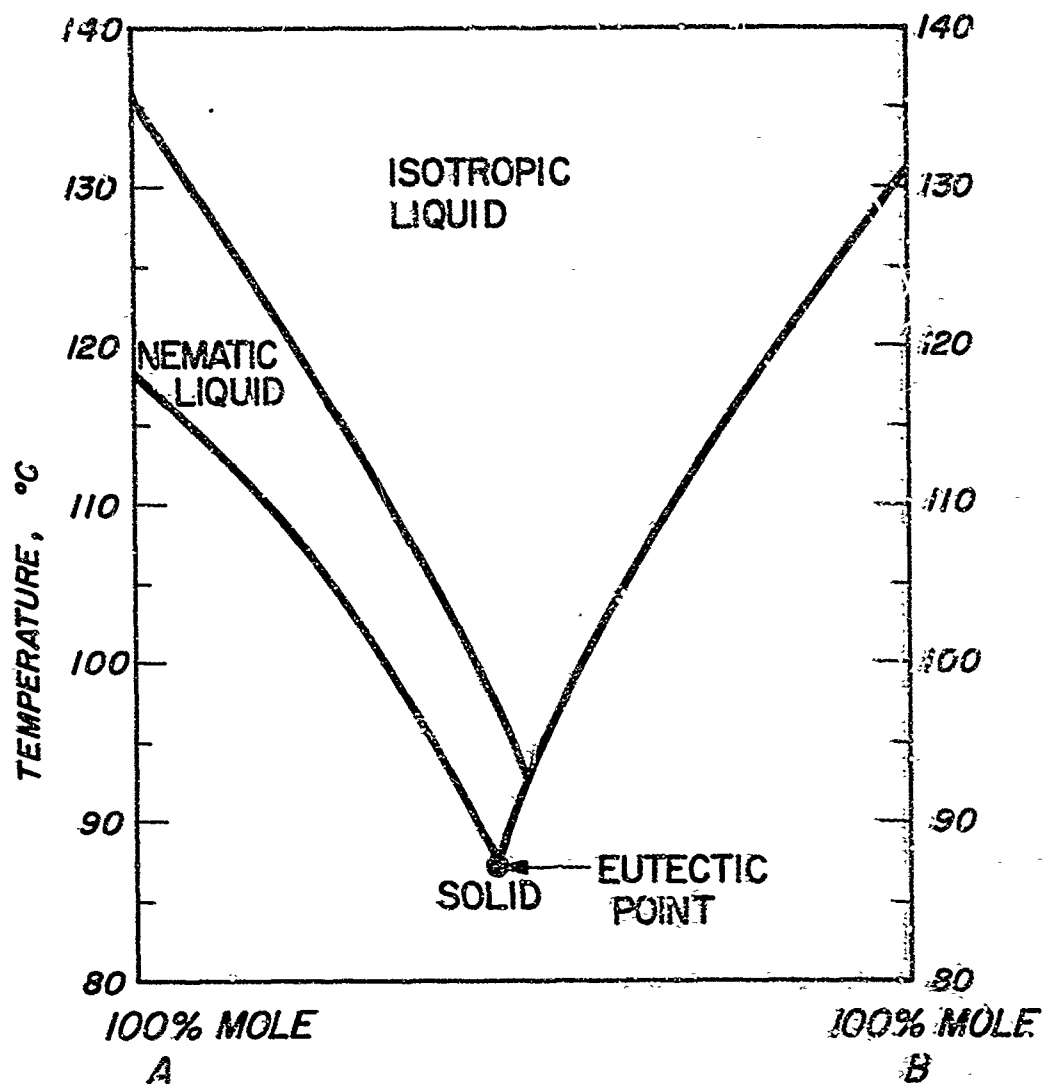


Figure 15. Phase diagram of binary mixture of nematic compound with non-mesomorphic compound.



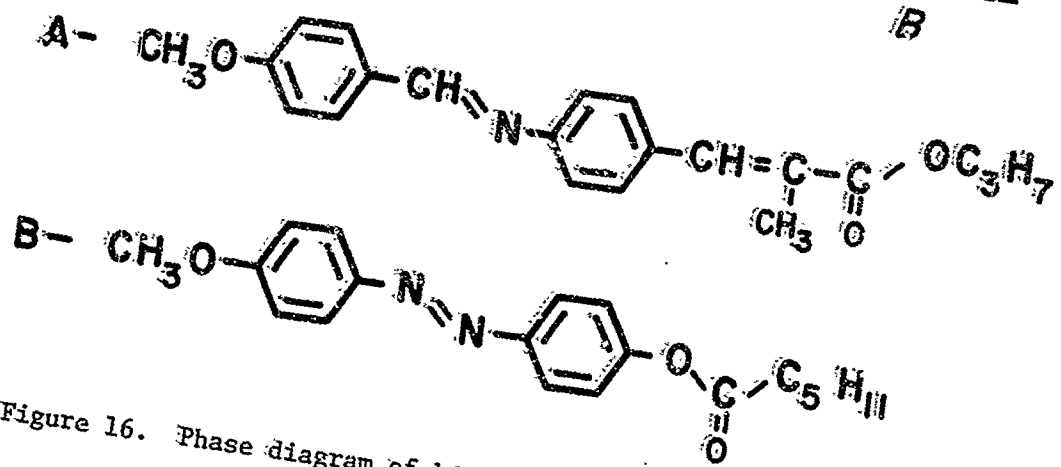
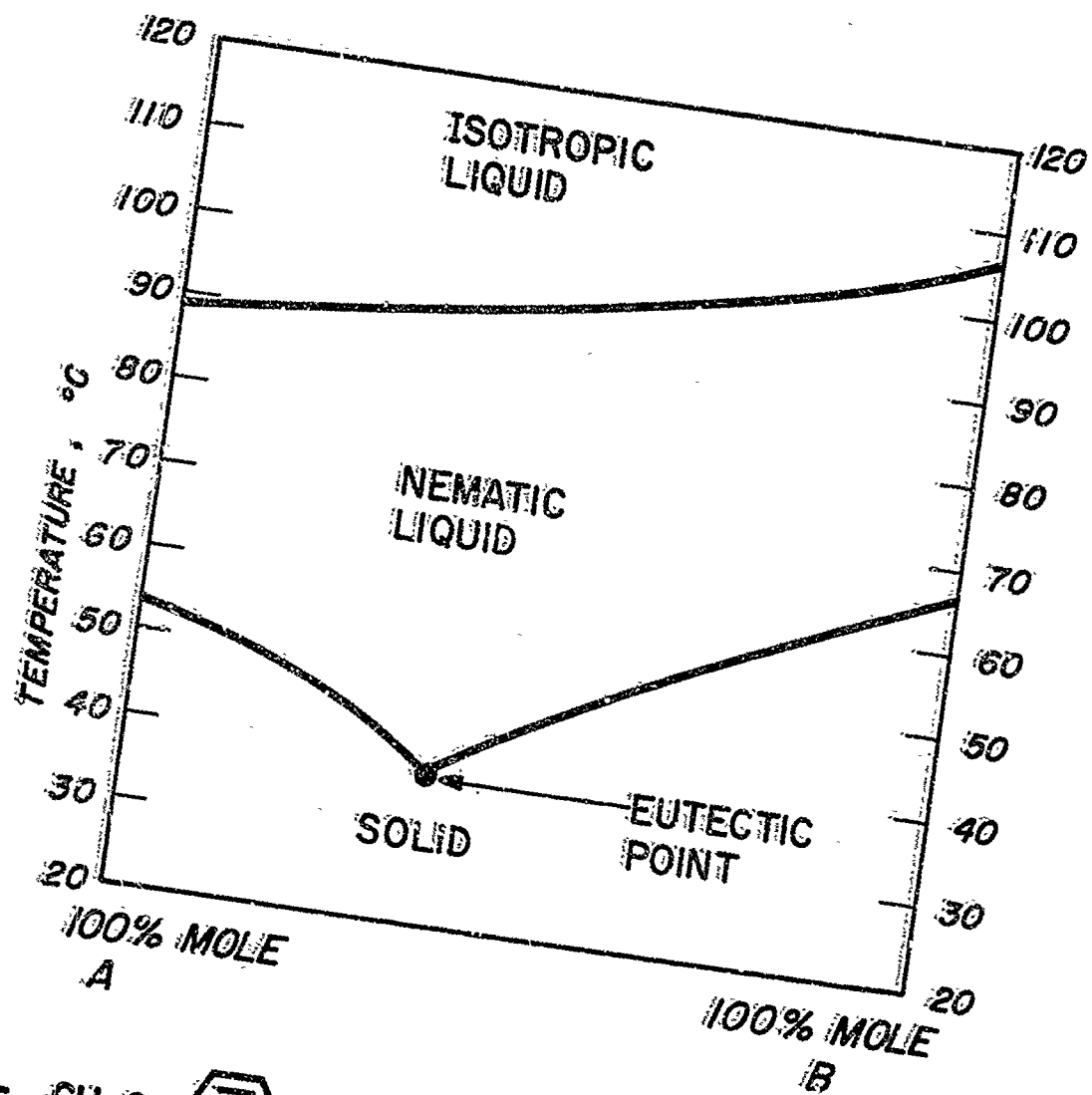


Figure 16. Phase diagram of binary mixture of nematic compounds.

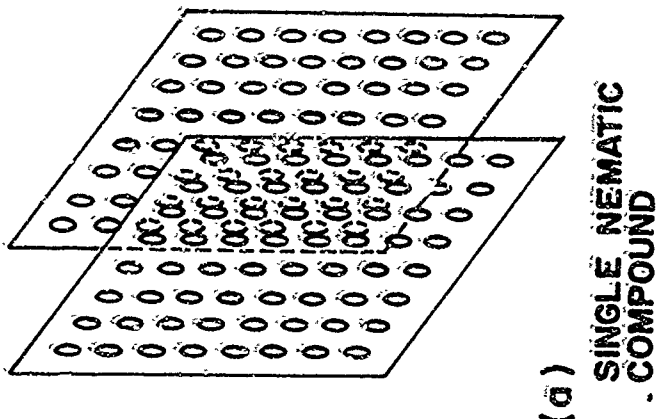
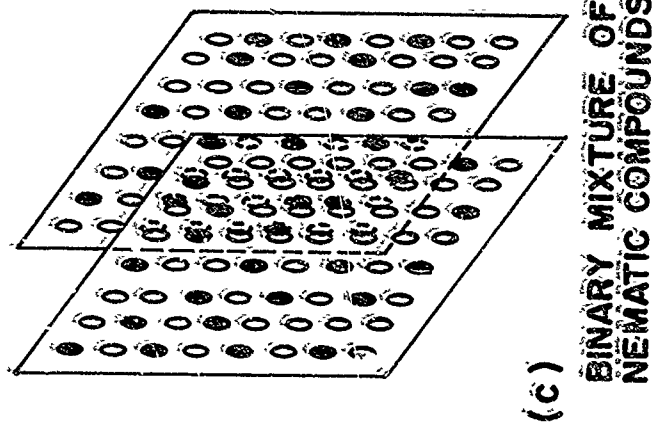
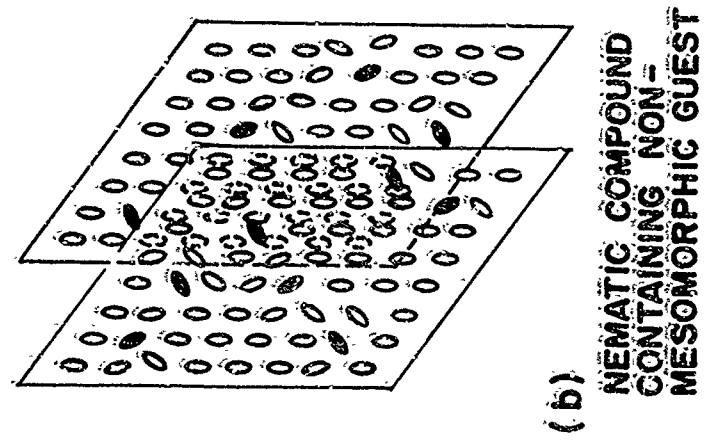


Figure 17. Structure of nematic mesophases.

TABLE VI

## Binary Mixtures of Carbonate Esters



A (R = C<sub>6</sub>H<sub>13</sub>), B (R = C<sub>7</sub>H<sub>15</sub>)

Mole %		Transition Temperatures, °C	
A	B	Crystal → Nematic	Nematic → Isotropic
100	--	44	84
90	10	41	84
80	20	38	82
70	30	37	79
60	40	35	77
50	50	33	74
40	60	27	73
30	70	28	71
20	80	34	68
10	90	35	67
--	100	36	54

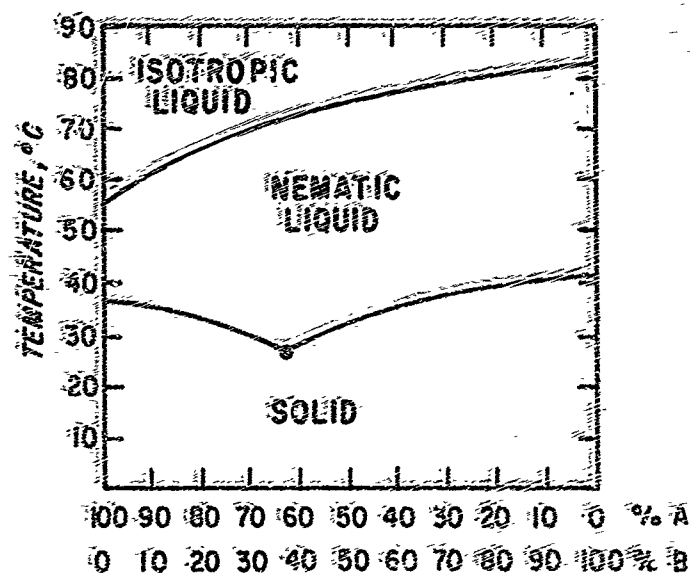
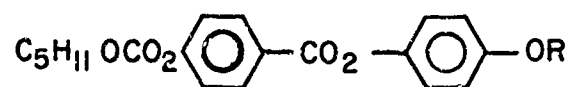


Figure 18. Binary phase diagram of mixtures taken from the series:  $\text{C}_{13}\text{H}_{27}\text{OCO}_2\text{C}_6\text{H}_4\text{CO}_2\text{C}_6\text{H}_4\text{OR}$  where R = C<sub>6</sub>H<sub>13</sub> (A) and C<sub>7</sub>H<sub>15</sub> (B).

TABLE III

Ternary Mixtures of Compounds Taken From the Series:



$$\text{R} = \text{C}_5\text{H}_{11} \text{ (A)}, \text{C}_6\text{H}_{13} \text{ (B)}, \text{C}_7\text{H}_{15} \text{ (C)}$$

Mole %			Transition Temperatures, °C	
A	B	C	Crystal → Nematic	Nematic → Isotropic
50	50	0	30	80
0	50	50	35	74
50	0	50	28	83
33	33	33	27	79
10	15	75	38	74
15	75	10	29	76
75	10	15	30	82
40	40	20	31	78
40	20	40	26	79
20	40	40	24	76
50	25	25	27	78
25	25	50	26	74
25	50	25	31	77

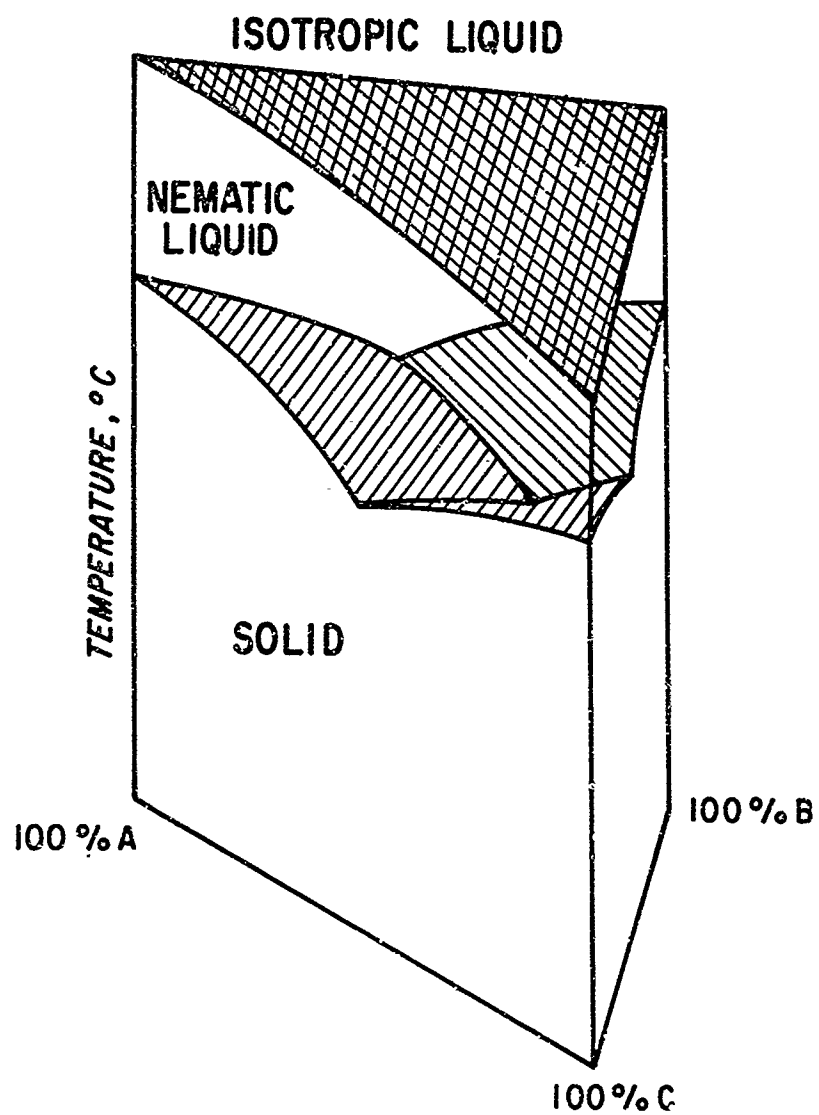


Figure 19. Ternary phase diagram of compounds 36(A), 37(B), and 38(C).

### SECTION III

#### ELECTRO-OPTICAL RESPONSE MEASUREMENTS

Measurements of the electrical characteristics and optical response behavior of electro-optic cells fabricated with one of the carbonato ester compounds (p-butylcarbonato-p'-ethoxyphenyl benzoate, compound 25) were carried out by procedures previously described[1]. The recorded data were taken with a 1/2-mil cell heated in air at approximately 55°C. Tin oxide coated plane-parallel quartz plates were used to make electrical contact and to contain the nematic material.

The initial resistivity of a freshly prepared cell was  $2 \times 10^{10}$  ohm-cm. Application of a high dc field (150 kV/cm) was necessary to achieve dynamic scattering due to domain formation in the liquid crystalline material. However, the efficiency of light scattering was considerably lower than that observed in other nematic materials. A rise time of 35 msec and a contrast ratio of 3:1 was measured for a 200-V dc addressing pulse. The natural relaxation time constant of this cell was about 100 msec. Much better results were obtained using a low-frequency ac signal. A 30-Hz gated signal at 120 V produced a highly efficient scattering system. However, higher frequencies required even higher voltages to produce light scattering and above 100 Hz no scattering at all was observed. Similar results were obtained with the room-temperature mixture described in Section II.

Two models have been suggested to explain the behavior of these materials under electric fields. In the first model the molecules of the nematic compound are oriented with their long axes perpendicular to the electrode surfaces (homeotropic behavior). This orientation presumably occurs as a result of the strong attraction between the carbonyl group and the tin oxide coating. Thus, between cross polarizers the light is extinguished. Application of an electric field produced a reorientation of the molecules such that they begin to align themselves with their dipole moments in the direction of the field. This process produces differently oriented regions of the birefringent material and light scattering occurs. If the polarity remains fixed (as with dc), the light scattering will be transient since scattering occurs only during the realignment process. However, if the polarity is reversed every 1/30th of a second, the molecules will be in dynamic realignment and light scattering will be continuous.

The second model assumes that impurity ions present in the material are rapidly swept to the electrode surfaces under dc excitation. The disruptive effect of ions in motion through the oriented nematic material gives rise to the transient scattering effect. Under ac excitation, however, the ions would be reversing their direction every 1/30th of a second and dynamic scattering would be observed.

We were unable to distinguish between these two models on the basis of available information. Further experiments will be required to elucidate the mechanism of this process.

Since these materials required higher voltage for operation than materials previously developed by RCA, we did not use these compounds in the display devices currently furnished under the contract. However, it is anticipated that fabrication of novel display units in the future will require materials with characteristics which these compounds exhibit.

## SECTION IV

### MECHANISM OF DYNAMIC SCATTERING IN NEMATIC LIQUID CRYSTALS

In these studies we concentrated on two problems: First, we investigated domains, in particular the underlying orientation patterns, in various nematic compounds. Second, we studied the generation of disclinations (= linear alignment discontinuities) in electric fields and their disappearance upon the removal of the field. The latter experiments were restricted to p-azoxyanisole because all of the material constants are known for this material.

#### A. DOMAINS

It is well known that conducting nematic liquid crystals do not always align in low-frequency electric fields in a direction of maximum polarizability. This is particularly true of those materials whose dielectric anisotropy is negative, such as p-azoxyanisole. (Negative dielectric anisotropy means that the dielectric constant parallel to the unique axis is smaller than that perpendicular to it.)

A few years ago Williams[12] reported that certain nematic liquid crystals, among them p-azoxyanisole, can adopt a periodic optical texture. The phenomenon is observed if an electric field is applied to transparent sandwich cells. The stripes or cigarlike entities constituting the pattern were named "domains". Similar periodic patterns were reported afterwards by a number of workers[13] on various materials; the sample thicknesses ranged from 6 to 500  $\mu$ .

Williams suggested ferroelectric molecular ordering as one possible explanation for domain formation. In his static model the unique axis of the nematic material is assumed to be polar and in directions parallel to the domain walls. Saupe[14] proposed a connection with material flow. A dynamic model would not contradict the nonpolarity commonly ascribed to the nematic order. A fairly complete theory of domain formation of the latter type has recently been developed by RCA[15]. Besides material flow, we employ such concepts as anisotropic conductivity and polarizability, space charge, and shear-induced and distortion torques acting on the unique axis.

Generally, the theory predicts that the domain width roughly equals the sample thickness at the threshold voltage of formation and that this voltage is independent of thickness. A threshold voltage of a few volts is calculated for p-azoxyanisole, the only case in which the required 12 material constants are known. In all three points there is agreement with experiment[12,13,16]. For the same material, the theory predicts not only the striped optical texture but the type of orientation pattern giving rise to it.



In order to detect the orientation pattern in p-azoxyanisole (nematic range 118-135°C) we did the following experiments, using sandwich cells made up of tin-oxide-coated glass plates and  $2.5 \times 10^{-3}$ -cm-thick teflon spacers. The novel feature was a uniform alignment of the unique axis parallel to the glass in the fieldless state. It was achieved by the familiar method of rubbing the glass, for instance with a cotton swab and some p-azoxyanisole as lubricant. The unique axis aligns parallel to the direction of rubbing, which was checked by observing the dichroism of the sample[17]. This and the other observations were made in transmitted light under a polarizing microscope.

With the many cells studied it was always found that the domains run perpendicular to the direction of the unique axis in the fieldless state. The photo of an example (Figure 20) shows scratches due to rubbing; it was taken when only part of the sample displayed domains, as was often the case near the threshold voltage. Linearly polarized light was used although the domains were visible without polarization. Both polarizers passed light whose electric vector vibrated in the direction of the unique axis in the fieldless state. If the pair was rotated by 90° the domains were not visible. It follows that the effect of the electric field consists in turning the unique axis into the direction of the field.

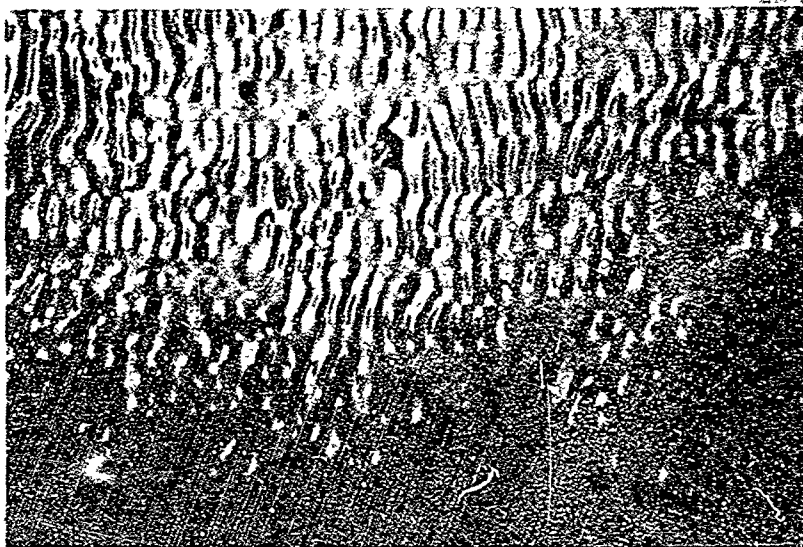


Figure 20. Incomplete domain texture of p-azoxyanisole as observed near the threshold voltage ( $\sim 3$  volts dc). Scratches indicating the direction of rubbing are seen in the lower part; total width of picture about 2 mm.

A periodically distorted orientation pattern which agrees with our observations and the common assumption of fixed boundary alignment is sketched in Figure 21. The optical anisotropy being positive[17], light coming from below emerges concentrated in the left half and diluted in the right half of the figure if its electrical vector vibrates in the plane of the drawing. (The light should be displaced without changing its direction.) An exact optical analysis of the actual orientation pattern would require collimated light.

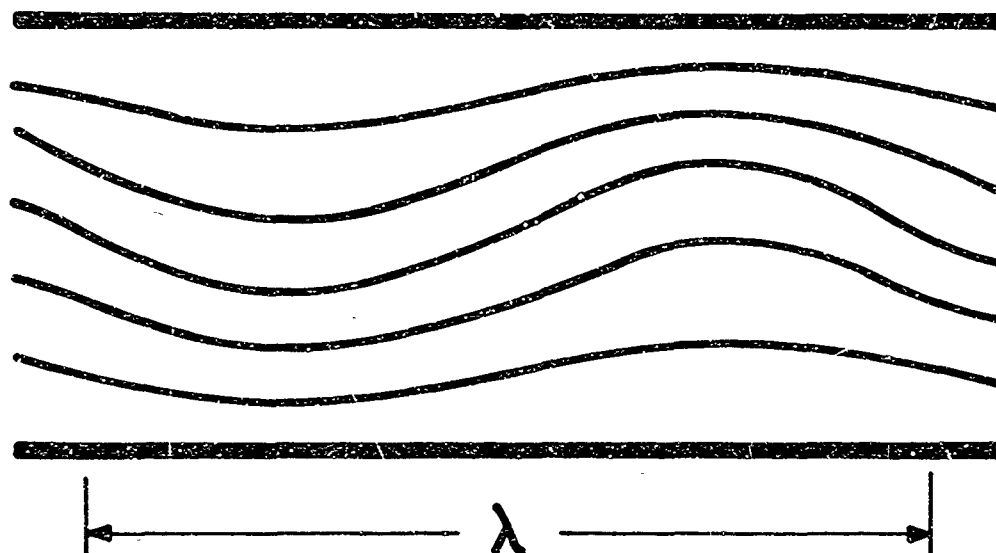


Figure 21. Periodically distorted orientation pattern as inferred from experiments. The local alignment is indicated by orientation lines (they are tangential to unique axis). The pattern represents a cross section perpendicular to the axes of the domains.

Periodic distortions like that sketched in Figure 21, whose "wave vector" is parallel to the unique axis in the undistorted state, are in accord with the aforementioned theory. Not surprisingly, the turbulence superseding the domains at higher voltages could be seen with both polarizer settings, which indicates stronger disturbances.

Domains and their orientation patterns were also studied on two other compounds. The samples were prepared as in the case of *p*-azoxyanisole, but the results were quite different. *N*-*p*-methoxybenzylidene-*p*-phenylazoaniline (nematic range 150-183°C) always showed a minority of domain walls which were more or less parallel to the direction of rubbing and which were seen in light whose electric vector was parallel to that direction. In *p*-anisaldazine (nematic range 169-181°C) domains were visible only if the electric vector was parallel to the direction of rubbing. This agrees with *p*-azoxyanisole but the long axes of domains usually were at  $\pm 45^\circ$  to the

direction of rubbing, often forming a rectangular network. Our theory of domain formation allows for more complicated patterns than the particularly simple one observed with and predicted for p-azoxyanisole. However, theory and experiment cannot be compared for other compounds because their material constants are not known.

## B. DISCLINATIONS

Nematic liquid crystals often are turbulent in a strong enough electric field. Because of its optical anisotropy a liquid crystal is comparable to a polycrystalline solid when it is turbulent. This explains why it scatters light (dynamic scattering). We studied the turbulent state with a view to finding nematic threads or disclinations. In our first experiments we used sandwich cells of the type employed for the generation of domains and dynamic scattering. Threadlike structures were indeed observed in nematic p-azoxyanisole under the microscope, forming small and irregular loops. The loops are constantly changing; they contract and vanish rapidly when the field is turned off. However, they tend to prolong the lifetime of the scattering state. Their control or prevention seem therefore desirable, at least at first sight.

In order to facilitate the observation of disclinations a second type of cell was used in all the following experiments, consisting of two uncoated glass plates separated by two parallel platinum wires which served both as spacers and electrodes. The wires were 50 to 250  $\mu$  thick and 1 to 2 mm apart. Nematic p-azoxyanisole filled the space between and beyond them. In contrast to the previous setup this geometry permitted the generation of large and relatively very long-lived disclination loops. Two contracting loops photographed a few seconds after turning off the field are shown in Figure 22. Applying a rising dc voltage we found loops to appear at about 30 V, preceded by bright areas at 10 V. Both were mostly mobile which suggests generation in the bulk. When the voltage was on, new loops were constantly forming and others contracting, the speed of formation rising with voltage. The decay time after switching off was independent of voltage, increased with thickness, and was 0.5 to 15 sec for average-sized loops. This demonstrates that threads may have a strong effect on the turn-off time in electro-optical effects.

In other experiments we used glass plates that were rubbed in one direction with a cotton swab before the cell was assembled. Otherwise, the setup was the same as before. The uniform wall alignment caused by the rubbing was perpendicular to the direction of the field. This appeared to prevent the formation of loops in the bulk. However, there was still a very effective generation at the electrode wires. When the field was turned off some loops were usually found which were not associated with the electrodes. Theory predicts that within a loop the alignment should rotate by an integer multiple of  $\pi$  as one goes from one glass plate to the other. This could not be proved directly, because in weakly twisted orientation patterns the light rotates with the unique axis. However, the enclosed areas were slightly yet distinctly darker than the rest of the cell. The only plausible explanation seems to be a twist of the orientation pattern.



Figure 22. Two contracting disclination loops, photographed a few seconds after removal of the generating electric field.

If the glass was not rubbed to produce uniform wall alignment, some disclinations attached themselves to one of the walls, forming straight or curved lines. A higher threshold voltage was needed for the attachment than for the generation in the bulk. Surface disclinations differed from those in the bulk by a thinner appearance, longer lifetime, and interaction with irregularities on the wall. Besides, they were frequently open-ended rather than closed loops. Often quasi-stationary remnants of these surface disclinations acted as nuclei for the formation of bulk disclinations when the voltage was turned on again. Wall disclinations were also observed many years ago in nonelectrical experiments[17]. It is not clear to us how they can be attracted by the wall without collapsing.

A special class of disclinations was generated in thick samples (ca. 10 mils). They were in the bulk but thicker than the regular bulk disclinations. Usually these disclinations did not form loops but branched into two disclinations of the normal, thinner variety. We suspect that around the thicker disclinations the alignment rotates by  $360^\circ$  while the rotation is  $180^\circ$  around the thinner ones. Our observation and interpretation are in line with similar branching phenomena observed by other workers in cholesteric liquid crystals relaxing from a stretched configuration (produced by a magnetic field) into their normal twisted state.

The formation energy of disclinations per unit length is unknown; it is infinite in the crudest theoretical approximation. The actual value depends on the composition of the core (central portion of disclination line) which sometimes is assumed to be isotropic. In an effort to see this core we developed a procedure to produce the so-called Schlieren texture in the nematic phase of p-azoxyanisole. Isotropic p-azoxyanisole was kept between

two glass plates without any spacers. The material was then rapidly cooled into the nematic state, with the borderline progressing from one side of the cell to the other. No electric fields were used. The orientation pattern corresponding to the Schlieren texture is characterized by a multitude of disclinations connecting and perpendicular to the glass plates of the sandwich cell. Observation in transmitted light under a polarizing microscope showed the cores to be much brighter than their surroundings, the brightness being rather independent of the setting of the polarizers. It was found that the core diameter is smaller than  $2 \mu$ . A satisfactory study of the core was not possible, at least not with the available microscope.

The study of the orientation pattern in domains indicates, as do other observations, that domains are associated with flow and thus a hydrodynamic phenomenon despite their static appearance. The turbulence and irregularity which start at about twice the threshold voltage of domain formation (in the cells used for "dynamic scattering") are associated with the formation of disclinations, at least in p-azoxyanisole. In the experiments with the field parallel instead of perpendicular to the glass plates we also observed a connection between turbulence and the generation of disclinations. These results seem to suggest that the breakdown of the domain pattern may result from the formation of disclinations in a sufficiently distorted orientation pattern. Further experiments are needed to check this hypothesis.

## SECTION V

### FABRICATION AND ENCAPSULATION

Some problems associated with the fabrication of electro-optic cells containing nematic liquid crystals are discussed in this section. In addition, the various techniques which were employed to effect hermetic sealing and encapsulation of these devices are presented.

Studies completed prior to the contract had indicated that liquid crystal cells degraded *under operation* much more rapidly (i.e., 5 times faster) when not protected from contact with the air. Tests made in a nitrogen ambient indicated that the operating life of the cell was proportional to the total amount of charge passed through the cell for a given material. For anisylidene-p-aminophenylacetate cell failure under dc operating conditions occurred after the passage of 12 coulombs per square centimeter. Thus, for a cell operating at a current density of  $6 \mu\text{A}/\text{cm}^2$  the life is

$$J\tau_{\text{LIFE}} = Q_{\text{LIFE}}$$
$$\tau_{\text{LIFE}} = \frac{12}{6 \times 10^{-6}} = 2 \times 10^6 \text{ seconds} = 555 \text{ hr}$$

For an operating current density of  $1 \mu\text{A}/\text{cm}^2$  the life would be 3330 hours. Operation under ac excitation in a nitrogen ambient yields lifetimes which are at least a factor of 25 greater. Thus, with the need for protecting cells from the air for longer operating life clearly established, several encapsulation schemes were conceived and evaluated.

Encapsulation of such a simple device structure at first glance seems straightforward. One immediately thinks of sealing the edges with an epoxy cement. This proved to be an unworkable solution due to chemical reaction between the curing epoxy and the liquid crystalline material resulting in an accelerated failure of the cell. Similar approaches using silicone cements were also unsuccessful for similar reasons. Of all the epoxies tested, "Torr-Seal", a low vapor pressure epoxy made by Varian Corp., gave the best results. Cells sealed using the material operated for 50 % of the life found in a nitrogen ambient.

The aforementioned technique involved sealing the cell with the liquid crystalline material in the cell. An alternative approach is to fabricate and seal the cell prior to the injection of the liquid through capillary tubes which are later sealed. Various glass frits (Owens Illinois, Vita) were tried as the sealing agent and fired prior to the injection of the liquid. While excellent seals were made using this technique (leak rate

$< 10^{-11}$  cc/sec) devices showed signs of decomposition after only 6% of the life measured in the nitrogen ambient and became inoperative after only 35%. These failures are probably attributable to products introduced into the cell during the firing of the glass frit. Since subsequent cleaning of the cell was not practical these byproducts remained in the cell and interacted with the liquid crystalline material when it was introduced.

Another sealing technique consisted of using a polyethylene gasket (1/2 mil thick) as both the cell spacer and encapsulant. Upon heating a cell containing the liquid crystal to 120°C the polyethylene gasket would soften and bond together the top and bottom pieces of glass which make up the cell. Initial problems with this technique centered about poor seals produced by rippling of the thin gasket. Subsequent seals involving slightly lower processing temperatures resulted in cells which had lifetimes superior to the previously discussed methods. The major disadvantage of this procedure, however, is that the thickness of the sealant cannot be greater than 1/2 mil, the necessary electrode separation. Large-area cells would be difficult to seal due to the tendency of the thin polyethylene gasket to ripple. Attempts using Mylar, Lexel, or Cellophane to replace polyethylene were unsuccessful due to interaction of these materials or impurities present in these materials with the liquid crystalline material.

The most useful and practical technique for encapsulation of liquid crystal devices involves a combination of the methods described above. Seals of this type were used in the state of the art devices provided under the contract (see Figures 25 and 28). In this method the bottom glass plate of the device is made slightly larger than the top. A glass box is bonded to the bottom plate (covering the top plate) by a polyethylene gasket seal. The glass-polyethylene seal is further reinforced with Torr-Seal. In order to remove traces of moisture, a small amount of desiccant was also encapsulated in the box. A schematic drawing of this encapsulation technique is shown in Figure 23. Cells made by this technique have shown no signs of degradation after 700 hours of continuous operation.

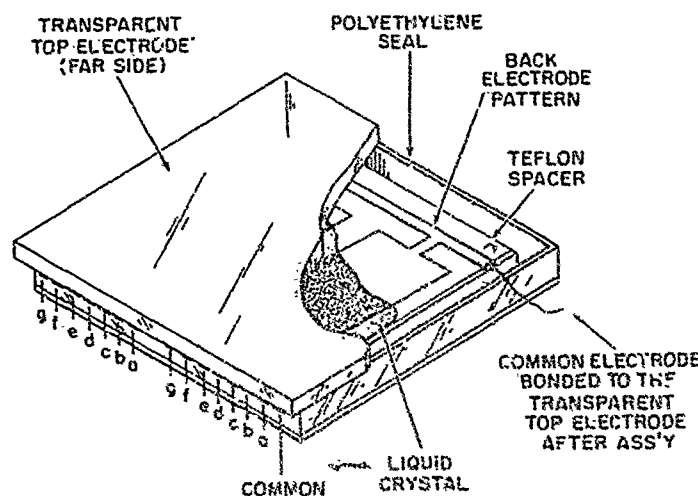


Figure 23. Assembled liquid crystal cell.

An investigation of transparent conductive coatings was also undertaken to study the quality of the various coatings and to determine which coating would be most suitable for liquid crystal display devices. Four different coatings were studied. They are:

- a. Sputter-deposited indium oxide on soft glass by PPG[20]
- b. Vapor-deposited tin oxide on FN glass by RCA
- c. Electropene (tin oxide) on soft glass by LOF[19]
- d. Electropene (tin oxide) on Dynasil by LOF[19]

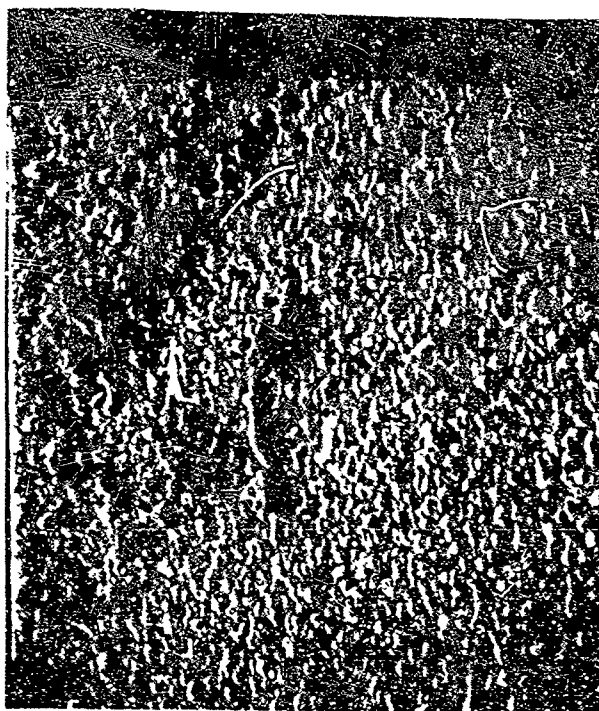
Sputter deposition of indium oxide on soft glass has the advantage of not warping the inexpensive soft glass during the coating process. However, the resultant coating is very soft and susceptible to scratches. Warping of the glass can be a serious problem because the 1/2-mil electrode separation must be maintained over the entire cell area in order to preserve field uniformity.

The vapor-deposited tin oxide on FN glass, which was prepared at RCA, resulted in warped plates. This warping was presumably due to the high temperature at which deposition occurred. In addition, the coating was found to be porous (determined by scanning electron microscopy, see Figure 24) and thus vulnerable to contamination. Similar results were obtained by LOF with vapor deposition of Electropene on soft glass.

This highest quality material obtained to date was, therefore, the Dynasil plates (synthetic quartz) with an Electropene coating prepared by LOF. The coating is smooth, uniform, and relatively rugged. Furthermore, little or no warping of the Dynasil plates occurs during vapor deposition. However, a major disadvantage to the use of Dynasil is the cost, which makes this material about an order of magnitude more expensive than soft glass.

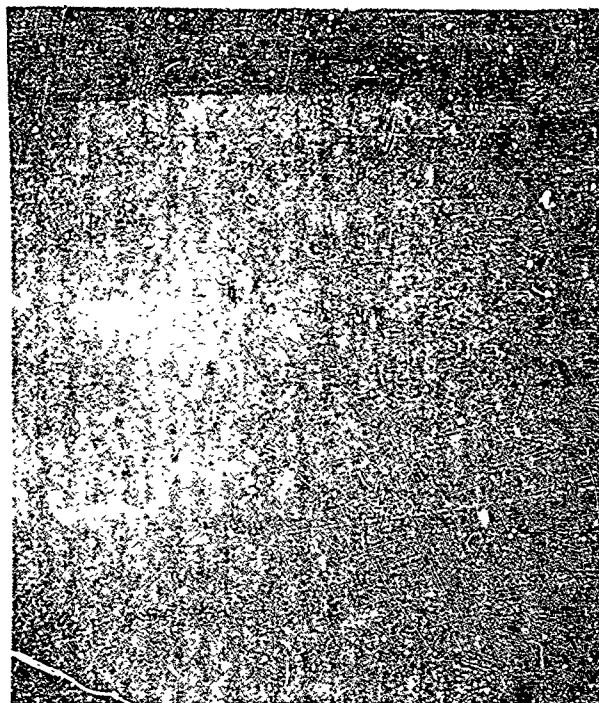
An ideal compromise between cost and quality would be to sputter-deposit tin oxide on soft glass. This was successfully accomplished on a small scale and appears to be an attractive technique for the preparation of these plates. Hence, we plan to purchase a large sputtering target for this purpose. The state-of-the-art devices prepared under this contract, however, were fabricated with either Electropene-coated Dynasil obtained from LOF or sputter-deposited indium oxide on soft glass obtained from PPG.





— 5 |  $\mu$  | 5 —

Vapor Deposited Coating



Sputtered Coating

Figure 24. Scanning electron microscope studies of transparent conductive coatings (Mag. = 10,000X).

## SECTION VI

### STATE-OF-THE-ART DEVICES

Several liquid crystal devices were fabricated and delivered to the contract monitoring officer. These included the following:

1. A two-digit *reflective* liquid crystal cell (2 in. x 2 in. x 3/8 in.) which was encapsulated by the glass box technique previously described. The cell was mounted on a printed-circuit board.

2. A two-digit transmission type liquid crystal cell (2 in. x 2 in. x 3/8 in.) which was also encapsulated by the glass box technique and mounted on a printed circuit board. A special louvered plastic (from 3M Company), which allows the transmission of light at only one angle, was attached to the back of the display. This results in improved contrast when the display is viewed with transmitted light since light is scattered in all directions at the points of electrical activation. The cell is shown in Figure 25.

3. An integrated driving circuit (Figure 26) which is capable of addressing one seven-segment numeric indicator. The output connectors in this package have been paralleled in order that both digits of the display may be activated simultaneously. The entire package is compact (2 in. x 4 in. x 1 in.) and contains a rechargeable battery (Figure 27).

4. A 4-in. x 4-in. transmission type liquid crystal cell encapsulated by the glass box technique and displaying a TV test pattern (Figure 28). The pattern was defined by standard photoetching processes. The display is activated by a rechargeable battery.

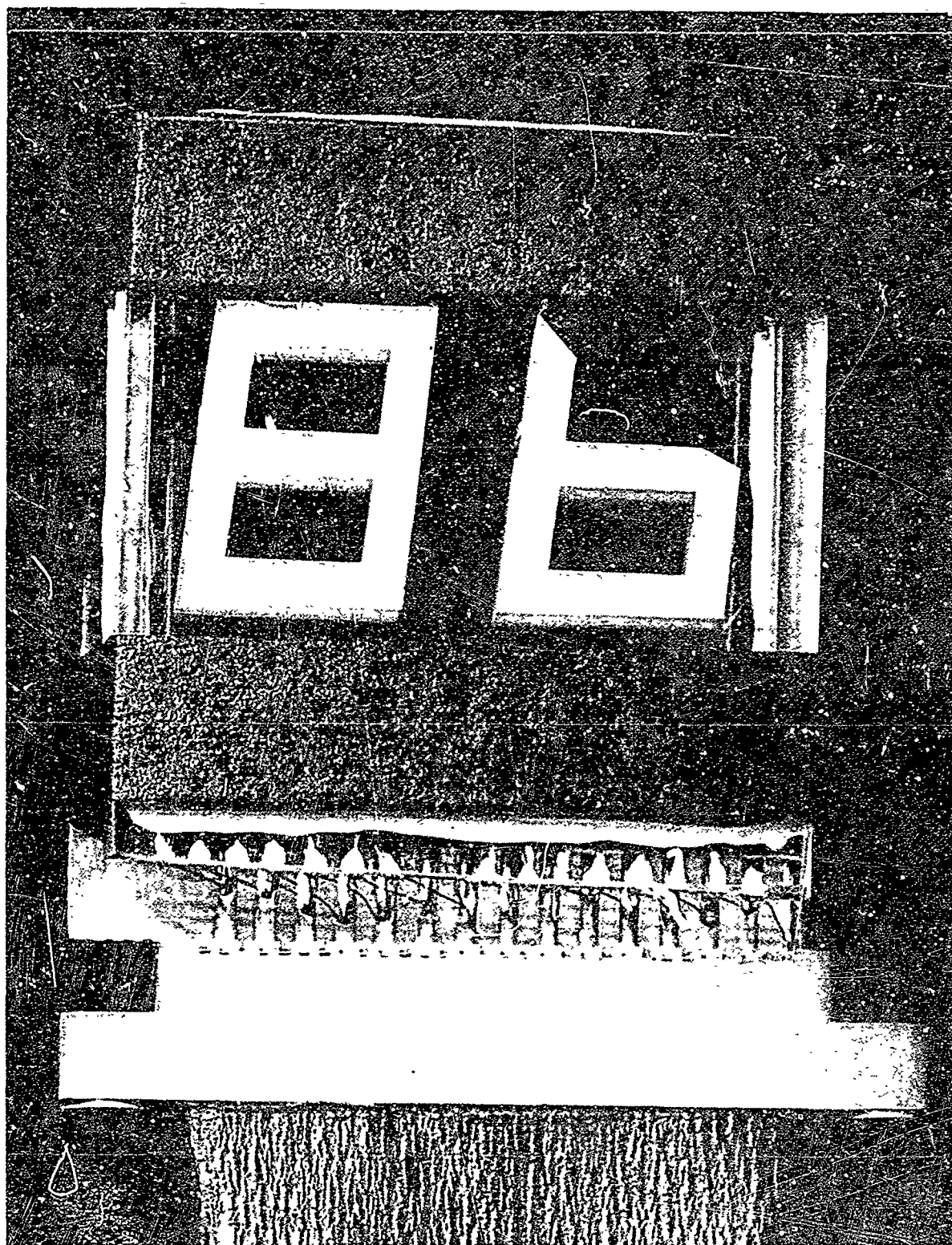


Figure 25. Two-digit transmission type liquid crystal cell.

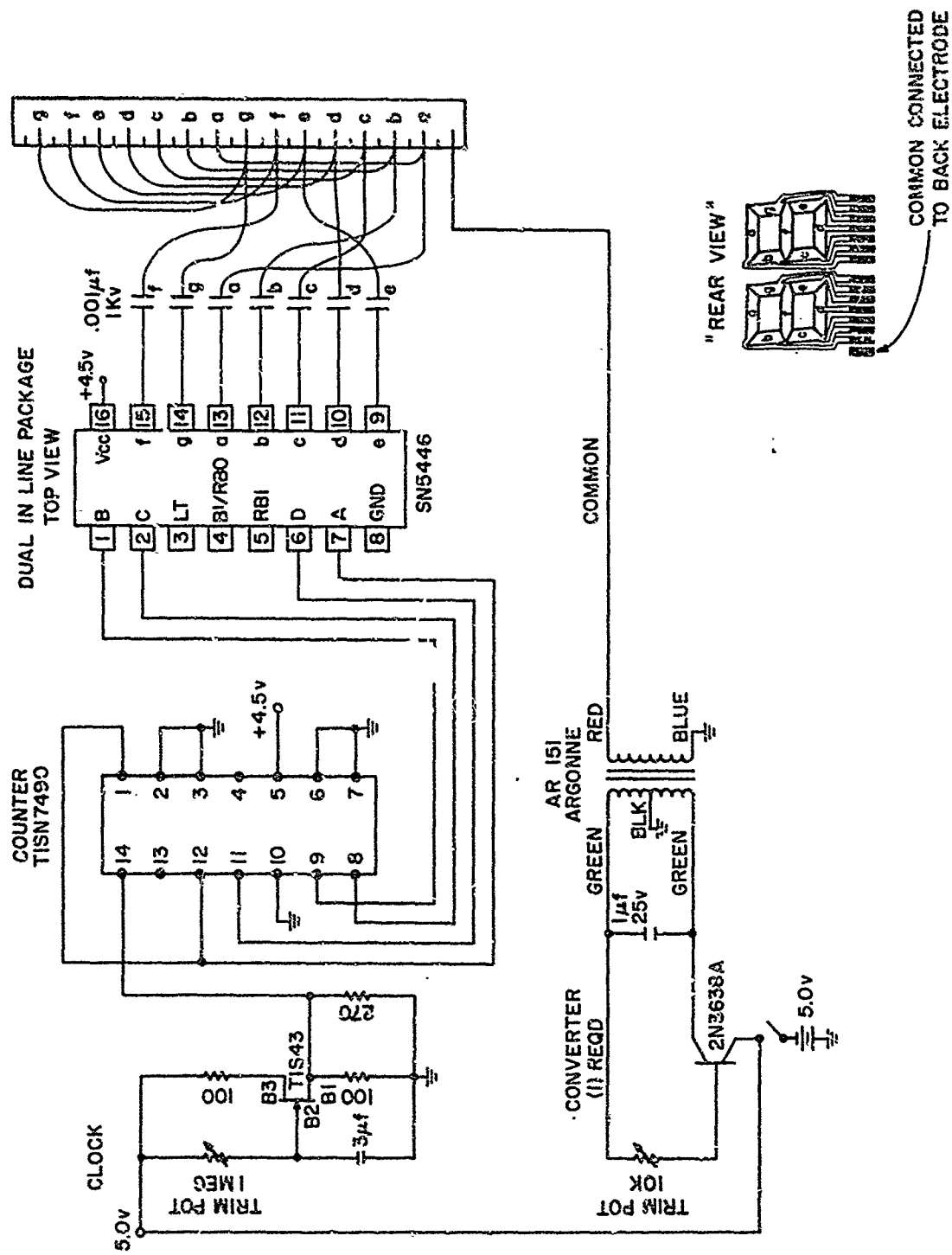


Figure 26. Schematic diagram of integrated driving circuit for seven-segment numeric indicator.

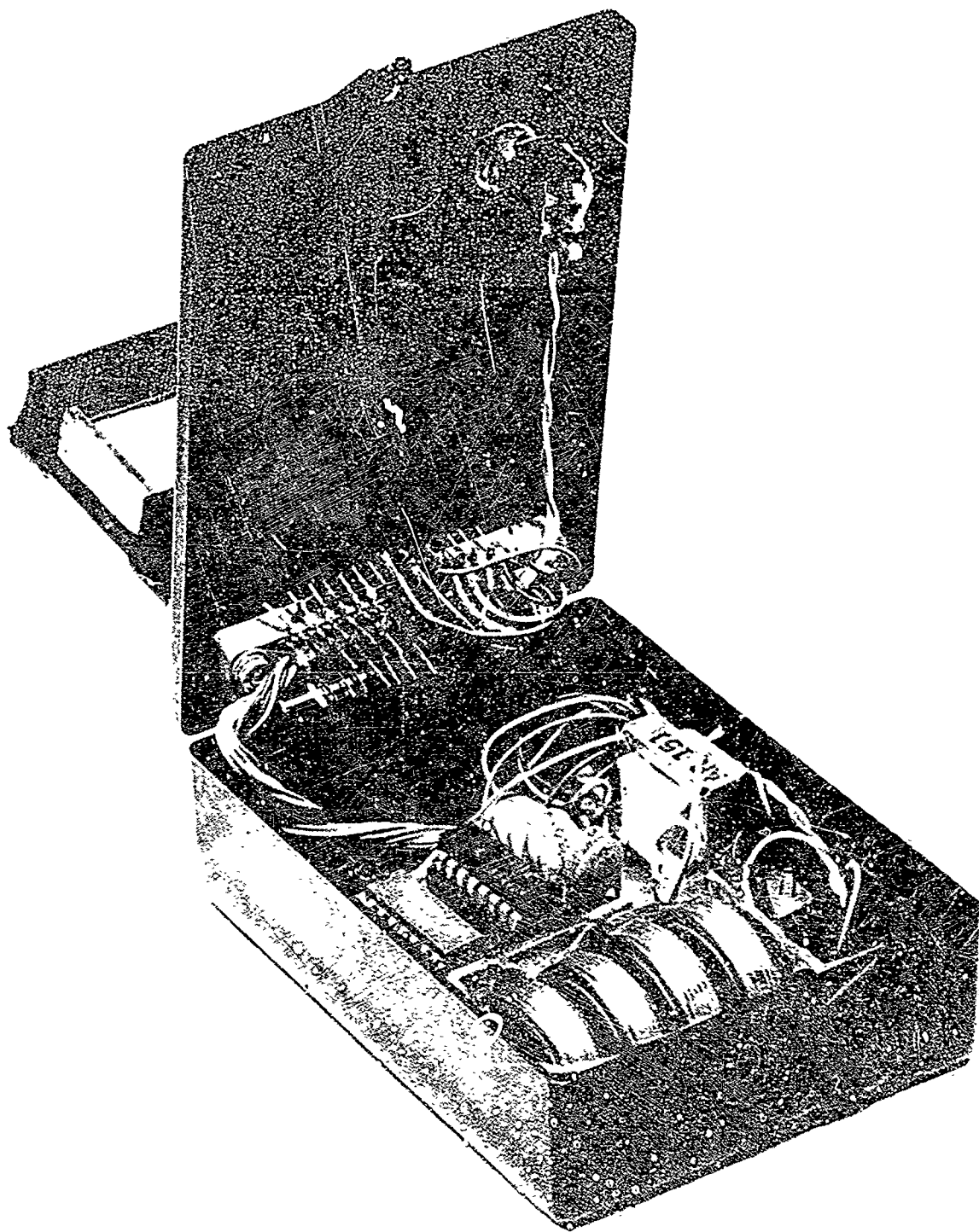


Figure 27. Numeric indicator with components exposed.

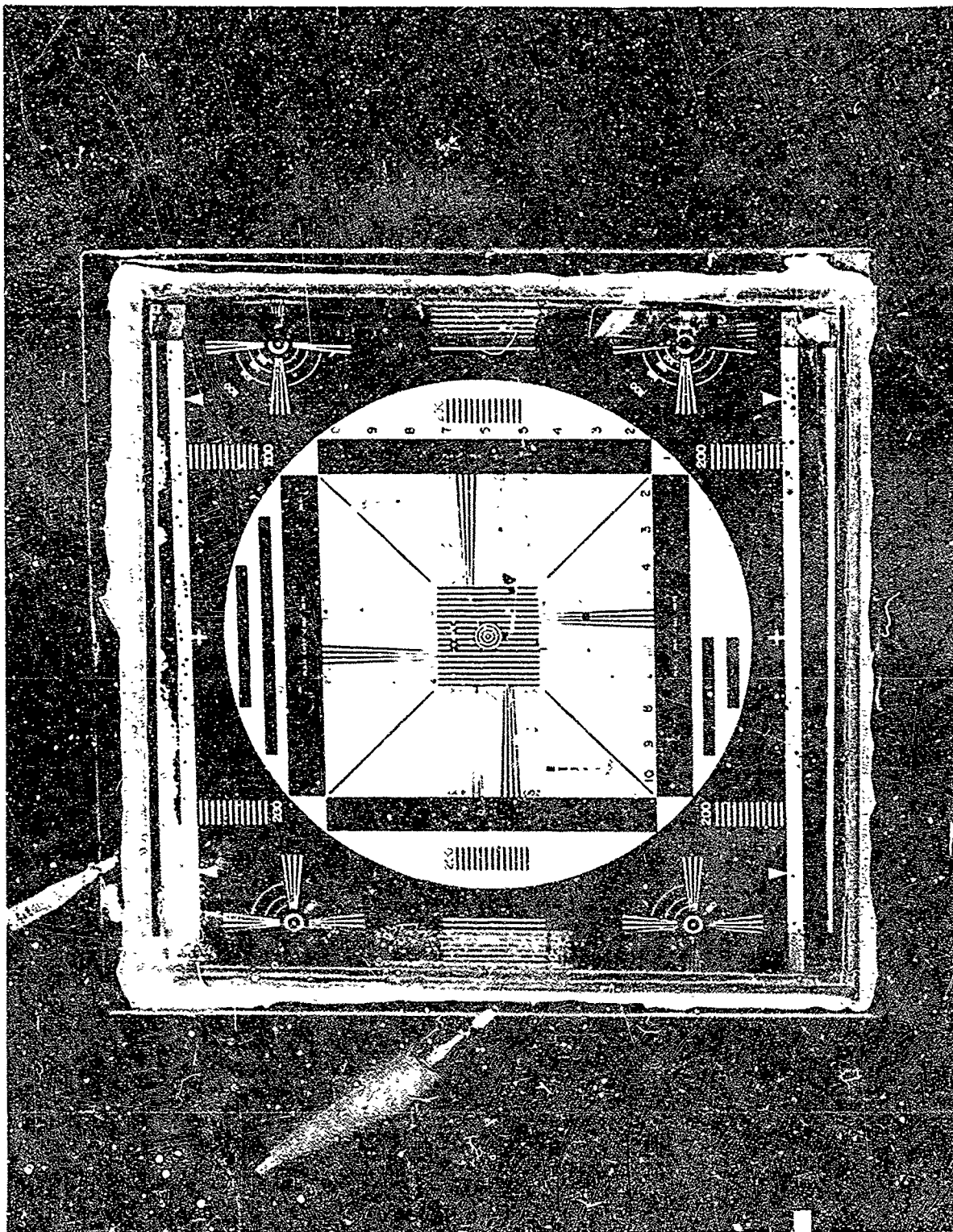


Figure 28. Transmission type liquid crystal cell displaying a TV test pattern.

## SECTION VII

### CONCLUSIONS

The development of a new series of room-temperature nematic materials has been achieved. This was accomplished through the use of mixtures of selected *p*-alkylcarbonato-*p*'-alkoxyphenyl benzoates. Compounds which contained from six to seven carbon atoms in both the ester and ether portion of the molecule gave the lowest melting points and widest nematic ranges. A number of binary and ternary mixtures of these materials exhibited nematic behavior at or near room temperature.

The carbonato esters were found to exhibit a highly efficient light-scattering effect with a 30-Hz gated signal at 120 V. However, this is about 100 V higher than that required to activate previously developed materials. Two mechanisms have been postulated to explain this behavior, but it has not been possible to distinguish between these two mechanisms.

An attempt to further elucidate the mechanism of dynamic scattering was made. The turbulence and irregularities present in liquid-crystalline materials which are in the dynamic scattering mode were found to be associated with the formation of disclination loops. Further experiments are needed to determine the origin and nature of these disclinations.

A glass-box technique has been developed for the sealing and encapsulation of liquid crystal display devices. Cells made by this technique showed no signs of deterioration after 700 hours of continuous operation with a gated ac signal.

This technique was used to fabricate two numeric indicators and a 4-in. x 4-in. transmission window displaying a TV test pattern.



## REFERENCES

1. G. H. Heilmeyer, L. A. Zanon, and L. A. Barton, Proc. IEEE, 56, 1162 (1968).
2. G. W. Gray, *Molecular Structure and the Properties of Liquid Crystals* (Academic Press, London, 1962).
3. G. H. Brown, W. G. Shaw, Chem. Rev., 57, 1049 (1957).
4. J. A. Castellano, J. E. Goldmacher, L. A. Barton, and J. S. Kane, J. Org. Chem., 33, 3503 (1968).
5. J. A. Castellano and J. E. Goldmacher, French Patent No. 1,537,000 (1968).
6. Eastman Organic Chemicals, Rochester, N. Y.
7. This criterion for purity has been established by Gray[2] and others.
8. B. L. Goydich and A. Murray performed these analyses. Satisfactory analysis was obtained for each compound.
9. We have found no significant difference between the transition temperatures obtained with this apparatus and that obtained by the differential scanning calorimetric technique.
10. J. S. Dave and J. M. Lohar, J. Chem. Soc. (London), 1967, 1473.
11. D. Demus, Z. Naturforsch., 22a, 285 (1967).
12. R. Williams, J. Chem. Phys., 39, 384 (1963).
13. A. P. Kapustin and L. S. Larionva, Kristallografiya, 9, 297 (1964) [Soviet Physics - Crystallography, 9, 235]; A. P. Kapustin and L. K. Vistin, Kristallografiya, 10, 118 (1965) [Soviet Physics - Crystallography, 10, 95]; G. Elliott and J. G. Gibson, Nature, 205, 995 (1965); G. H. Heilmeyer, J. Chem. Phys., 44, 644 (1966); R. Williams, Advances in Chemistry Series, 63, 68 (1967); P. Kassubek, quoted in Ref. 14; L. K. Vistin and A. P. Kapustin, Optika i Spektroskopiya, 24, 650 (1968) [Optics and Spectroscopy, 24, 348]; L. K. Vistin and A. P. Kapustin, Kristallografiya, 13, 349 (1968) [Soviet Physics - Crystallography, 13, 284].
14. A. Saupe, Angew. Chemie internat. Ed., 7, 97 (1968) (review article).
15. W. Helfrich, J. Chem. Phys., 51, 4092 (1969).
16. G. H. Heilmeyer (private communication) confirmed that the threshold voltage does not depend on sample thickness, for p-azoxyanisole and the range  $6 \cdot 10^{-4}$  -  $5 \cdot 10^{-3}$  cm.
17. See, e.g., I. G. Chistyakov, Usp. Fiz. Nauk, 89, 563 (1966) [Soviet Physics -- Uspekhi, 9, 551 (1967)] (review article).



REFERENCES (Continued)

18. W. Helfrich, J. Chem. Phys., 51, 2755 (1969).
19. Libby-Owens Ford, Liberty Mirror Div., Brackenridge, Pa., 19422.
20. Pittsburgh Plate Glass Co., Glass Research Center, Pittsburgh, Pa., 15238.
21. Dynasil Corporation, Berlin, N.J. 08009. This material is 1/8 in. quartz.

UNCLASSIFIED

Security Classification

DOCUMENT CONTROL DATA - R & D		
Security classification of title, body of abstract and indexing annotation must be entered when the overall report is classified		
1. ORIGINATING ACTIVITY (Corporate author)		2a. REPORT SECURITY CLASSIFICATION
RCA Corporation RCA Laboratories Princeton, New Jersey 08540		Unclassified
3. REPORT TITLE		2b. GROUP
FIELD EFFECT LIQUID CRYSTAL		N/A
4. DESCRIPTIVE NOTES (Type of report and inclusive dates)		
Final Report 19 December 1968 - 18 December 1969		
5. AUTHOR(S) (First name, middle initial, last name)		
Joseph A. Castellano      Michael T. McCaffrey      Ronald N. Friel Joel E. Goldmacher      Lewis A. Zanoni      Allan Sussman Wolfgang H. Helfrich      Edward F. Pasierb, Jr.		
6. REPORT DATE	7a. TOTAL NO. OF PAGES	7b. NO. OF REFS
June 1970	47	21
8a. CONTRACT OR GRANT NO.		9a. ORIGINATOR'S REPORT NUMBER(S)
F30602-69-C-0142		
b. PROJECT NO.		9b. OTHER REPORT NO(S) (Any other numbers that may be assigned this report)
5597		
c. Task No.		
559704		
d.		RADC-TR-70-96
10. DISTRIBUTION STATEMENT		
This document is subject to special export controls and each transmittal to foreign governments or foreign nationals may be made only with prior approval of RADC (EMBDE), GAFB, NY 13440.		
11. SUPPLEMENTARY NOTES		12. SPONSORING MILITARY ACTIVITY
		Rome Air Development Center (EMBDE) Griffiss Air Force Base, New York 13440
13. ABSTRACT		
<p>A new series of nematic liquid crystals based on p-alkylcarbonato-p'-alkoxyphenyl benzoates was prepared. Binary and ternary mixtures of selected derivatives taken from this series exhibited nematic behavior at or near room temperature. These materials were found to exhibit a highly efficient scattering system with a gated ac signal at 120 V. A study of the orientation pattern of domain formation and the generation of disclination loops was undertaken in an effort to further elucidate the mechanism of dynamic scattering. A practical and useful technique for the sealing and encapsulation of liquid crystal cells was developed. This procedure was applied to the fabrication of two numeric indicators and a transmission window which were furnished under the contract.</p>		

DD FORM 1 NOV 65 1473

UNCLASSIFIED

Security Classification

UNCLASSIFIED

Security Classification

14. KEY WORDS	LINK A		LINK B		LINK C	
	ROLE	WT	ROLE	WT	ROLE	WT
Field effect liquid crystals Liquid crystals Disclination loops Nematic compounds Electro-optic effects Dynamic scattering						

UNCLASSIFIED

Security Classification

SAC--Griffiss AFB NY 4 Jul 70-85

END